Genome-wide association for loci influencing thermal performance curves in *Neurospora crassa*

Emmi Räsänen[1], Neda N. Moghadam[1], Karendeep Sidhu[1],
Pauliina A. M. Summanen[1], Henna-Riikka Littunen[1], Tarmo Ketola[2],
Ilkka Kronholm[1]

[1]Department of Biological and Environmental Science, University of Jyväskylä, FI-40014 Jyväskylä, Finland

[2]Department of Forest Science, University of Helsinki, FI-00014 Helsinki, Finland

Running Head: Genetics of thermal performance curves

Keywords: allelic effects, fungi, genetic architecture, growth rate, nested association mapping, temperature, trade-off

Corresponding author:

Ilkka Kronholm

Department of Biological and Environmental Science,

University of Jyväskylä,

P.O. Box 35, FI-40014

Jyväskylä,

Finland

Fax +358 14 617 239

Email: ilkka.kronholm@jyu.fi

Abstract

Temperature poses a unique challenge to ectothermic species, as it affects all biochemical reactions in the cell and causes physiological stress. The effect of temperature on an organism can be described by a thermal performance curve (TPC), which displays organismal performance, such as growth rate, as a function of temperature. Previous studies on thermal performance have revealed different amounts of genetic variation and trade-offs in TPC shape and position within species and populations. However, very little is known about the genetic architecture of TPCs on the level of individual loci and alleles. What is the identity of loci contributing to genetic variation in TPCs, and do the alleles exhibit trade-offs or thermodynamic scaling across species' tolerance range? We investigated the genetic architecture of thermal tolerance on the level of individual loci in the filamentous fungus *Neurospora crassa*. We used genome-wide association mapping to find loci influencing growth rate at different temperatures and TPC characteristics. We also evaluated the directions and magnitudes of allelic effects to investigate possible trade-offs. We observed both unique associations at specific temperatures, as some loci affected growth rate only at low, intermediate, or high temperatures, and associations that were shared across multiple temperatures. However, only weak evidence of trade-offs was detected, indicating that the evolution of TPCs in *N. crassa* is not constrained by allelic effects in opposite directions at hot and cold temperatures. Our findings indicate that variation in TPCs does not mainly depend on trade-offs.

Introduction

Among all of the abiotic stress factors, temperature poses a unique challenge for ectothermic organisms as temperature affects the stability of proteins and all biochemical reactions in the cell (Schulte, 2015; Arcus *et al.*, 2016). Therefore evolutionary adaptation to higher temperatures may be more difficult than to other abiotic stresses. This is especially concerning today as global temperatures are increasing as a result of greenhouse gas emissions (IPCC, 2013). As some organisms may have no possibility to migrate into colder areas, they have to adapt to higher temperatures, or otherwise they may perish (Deutsch *et al.*, 2008; Dillon *et al.*, 2010; Araújo *et al.*, 2013; Merilä and Hendry, 2014).

The response to temperature an ectothermic organism exhibits is called a thermal performance curve (TPC) (Huey and Kingsolver, 1989, 1993). This curve describes an aspect of organism's performance, such as growth or fitness, as a function of temperature. Often TPCs are skewed towards colder temperatures, and they have an optimum temperature, after which performance rapidly falls at higher temperatures (Sinclair *et al.*, 2016). As different species have TPCs with different optima and shapes (Maclean *et al.*, 2019; Kontopoulos *et al.*, 2020), genetics of the organism must be important for determining the TPC shape. Generally, most studies have detected genetic variation in thermal performance within species, although the extent of this variation differs between species and populations (Krenek *et al.*, 2011; Logan *et al.*, 2018, 2020; Martins *et al.*, 2019; Moghadam *et al.*, 2020; Querns *et al.*, 2022). Genetic variation is mostly restricted to certain aspects of temperature performance, for example, many studies report that majority of genetic variation is in TPC elevation rather than in the shifting optimum temperature (Shama *et al.*, 2011; Klepsatel *et al.*, 2013; Latimer *et al.*, 2015; Bartheld *et al.*, 2017; Moghadam *et al.*, 2020). However, a meta-analysis of selection experiments has revealed evidence of trade-offs when a population adapts to a new temperature optimum (Malusare *et al.*, 2023).

Since the activation energy of every biochemical reaction in the cell scales with temperature, thermodynamic effects must also influence the characteristics of TPCs (Angilletta *et al.*, 2010; Asbury and Angilletta Jr., 2010). Thermodynamic constraints and trade-offs are expected to affect

the evolution of species' thermal performance since the enzymatic reactions slow down at colder temperatures (Kontopoulos *et al.*, 2020). Conversely, the rate of biochemical reactions and also the organism's performance should be higher at warmer temperatures. Based on this specialisation and thermodynamics, cold-adapted species should have lower fitness at warmer temperatures and vice versa, which is observed as a optimum-shift between colder and warmer temperatures in TPCs (Malusare *et al.*, 2023). Cold-adapted species could also be constrained in their ability to enhance performance to the same level as warm-adapted species through evolution, unless there is a shift towards higher temperatures in TPC, also know as the "hotter is better" hypothesis (Angilletta *et al.*, 2010). The evidence for thermodynamic constraints is mixed, as some studies have reported larger effects (Frazier *et al.*, 2006; Sørensen *et al.*, 2018), and others only minor effects (Kontopoulos *et al.*, 2020; Malusare *et al.*, 2023).

While the genetics of TPCs has been investigated with quantitative genetic methods and QTL studies that have a low mapping resolution (Latimer *et al.*, 2015), we understand the effects of individual genes on TPCs poorly. What is the identity of genes that influence TPCs? How do allelic effects scale with temperature? For example, are there loci for which allelic effects scale thermodynamically, and other loci that affect growth only at specific temperatures? Moreover, the theory of TPC evolution often assumes that there are trade-offs between performance at higher and lower temperatures (Angilletta Jr., 2009; Angilletta *et al.*, 2010), but can this be observed on the level of genes or alleles?

In order to better understand the genetic architecture of TPCs, we performed a genome-wide association study for growth rate at different temperatures in the filamentous fungus *Neurospora crassa*. This ascomycete fungus is a genetic model system with both asexual and sexual life cycle (Roche *et al.*, 2014). It can be propagated clonally through asexual spores, or mating can be induced between individuals of different mating types. In nature, *N. crassa* is a subtropical species, that decomposes dead plant material. We used strains collected from Southeastern United States and the Caribbean (Ellison *et al.*, 2011; Palma-Guerrero *et al.*, 2013), and made crosses among some of the strains to generate a nested association mapping population. We have previously investigated

the genetic variation in TPCs for this population on the phenotypic level (Moghadam *et al.*, 2020), and here we use genotypic information for these lines to map loci that influence growth at different temperatures.

Materials and methods

Neurospora crassa strains

For nested association mapping, we used the strains described in Moghadam *et al.* (2020). Briefly, the strains used in this study included natural strains collected from Lousiana (USA), Caribbean, and Central America (Ellison *et al.*, 2011; Palma-Guerrero *et al.*, 2013). Sampling locations are shown in figure S1. We have made crosses between some of the natural strains to create additional lines for nested association mapping (Table 1). Strains belonging to a particular family are F_2 offspring of the parents. In total there were 434 strains in this study. Full list of the strains is presented in Supplementary Table S1.

Table 1: Strains for nested association mapping panel used in this study. FGSC = Fungal Genetics Stock Center.

Population	n	Parents	Source
Natural strains	118	–	FGSC
Family A	94	10948 × 10886	(Moghadam *et al.*, 2020)
Family B	50	10932 × 1165	(Moghadam *et al.*, 2020)
Family C	50	4498 × 8816	(Moghadam *et al.*, 2020)
Family D	52	3223 × 8845	(Moghadam *et al.*, 2020)
Family G	70	10904 × 851	(Moghadam *et al.*, 2020)
Total	434	–	–

Genotyping

A dense genotyping is needed for association mapping, but high density SNP chips are not available for *N. crassa*, and sequencing the genomes of all the 316 offspring from the families generated by crosses was not possible. Therefore, we employed a strategy where we used a full genome

sequencing data only for the 118 natural strains. Then we used a RAD-sequencing (Baird *et al.*, 2008) to obtain a moderate number of SNP genotypes for each offspring. We could then use the RAD markers to find the locations of recombination breakpoints. Because we know the full genome sequences of the parents, we could then infer the genome sequences for the offspring based on their RAD markers.

Genome re-sequencing of strains from natural populations

Some of the strains from natural populations had already been sequenced in previous studies, 23 strains had been sequenced by Zhao *et al.* (2015), 33 strains by Villalba de la Peña *et al.* (2023), and 61 strains were sequenced in this study. Including the reference genome of strain 2489, this comes to 118 re-sequenced strains.

We used the same methods for DNA extraction, sequencing and SNP calling as in Villalba de la Peña *et al.* (2023). Briefly, DNA was sent to Novogene (Cambridge, UK) for sequencing, using Illumina 150 bp paired-end reads. Reads were mapped against the reference genome (version 12) using BWA-MEM (Li, 2013). SNPs were called using Haplotypecaller in GATK (McKenna *et al.*, 2010), and filtered using Wormtable (Kelleher *et al.*, 2013) and custom python scripts. For a SNP to be included it had to have read depth ≥ 5 in the focal sample, and mean ≥ 5 across all samples. The same procedure was used with genotype quality ≥ 30, and mapping quality ≥ 40. We performed genotyping in a diploid mode, even if *N. crassa* is a haploid, and excluded heterozygous sites. Based on our experience the heterozygous sites in a haploid organism are likely to represent read mapping problems, see also Kronholm *et al.* (2017). If a site did not pass the filters for a given sample, the genotype of that sample was assigned as missing data. See methods in Villalba de la Peña *et al.* (2023) for details.

RAD-sequencing

We genotyped the 315 offspring of the crosses by using a RAD-sequencing method (Baird *et al.*, 2008). We extracted DNA from the strains with phenol-chloroform extraction and sent the samples

for RAD-sequencing by Floragenex Inc. (Oregon, USA). The sequencing was done by using a single digest with Pst I, barcode multiplexing, and Illumina sequencing with 100 bp read length.

The RAD-reads were cleaned and demultiplexed with the STACKS program (Catchen *et al.*, 2011). Across all RAD-samples 94.6% of the reads were retained after filtering low-quality reads or the ones were barcode could not be identified. Reads were aligned to the *Neurospora crassa* reference genome version NC12 using BWA-MEM (Li, 2013), and the resulting bam files were sorted with samtools. We added read groups and performed indel realignment with GATK (McKenna *et al.*, 2010) to parents and offspring of each family together, and then used Unified Genotyper in GATK for genotype calling with parameters: heterozygosity = 0.001, ploidy = 2, and minimum base quality score = 10. The resulting vcf files were processed using custom R scripts. For each family, we filtered out loci that had less than 20 individuals genotyped, loci that had genotype quality < 30, mean read depth ≤ 10 across the family, minor allele frequency ≤ 0.2, or had an unbalanced allelic depth ratio (log of ratio smaller than -1 or larger than 1). Further criteria included that at least one of the parents was genotyped and parental genotypes were different, neither parent was called heterozygous, and proportion of individuals called as heterozygous was < 0.1. For the remaining loci, all genotype calls with read depth ≤ 5 were set to missing data. There were also some loci that had been called as both a SNP and an indel, at the same position. In these cases only the indels were kept, as these polymorphisms likely represented complex mutations. After quality filtering there were 14445 loci left for family A, 13523 loci left for family B, 17297 loci left for family C, 16314 loci left for family D, and 11261 loci left for family G.

Criteria for filtering RAD loci was assessed by constructing genetic maps for each family using the R package ASMap (Taylor and Butler, 2017). We used the kosambi mapping function, and a p-value cut off of 10^{-6} for evidence of linkage. We observed that leaving markers with bad quality in the dataset produced genetic maps with excessive numbers of double cross-overs, or large local segregation distortion resulting from genotyping errors. For the filtered dataset some double cross-overs were still observed (Figure S2), while it is possible that some were due to genotyping error, most are likely real events. Marker order was generally concordant with the reference genome

(Figure S3).

Inference of full SNP genotypes for the offspring

Eleven to seventeen thousand markers obtained with RAD sequencing is not enough for high resolution association mapping, but they allowed us to identify the locations of recombination events in the offspring genomes. We used this information about recombination breakpoints to infer the genotypes of the offspring for all of the SNPs genotyped for the natural strains. For each offspring we classified its genome into segments inherited from the two different parents (e.g. Figure S4), SNPs for chromosome ends were classified according to the first or the last RAD-marker. Where recombination breakpoints occurred, those SNPs falling between the two RAD-markers flanking the breakpoint were set as missing data. Because some individuals had a lot of missing data for the RAD-markers, we used a conservative approach and segments where data was missing for the RAD-markers were inferred as missing for the SNP genotypes. The median distance between two RAD markers flanking the recombination breakpoints was 11.5 kb. Because *N. crassa* is haploid and the parent genotypes are known, there is no ambiguity in inferring the genotypes of the offspring due to heterozygosity or phasing issues. After inferring offspring SNP genotypes, we created the final genotype dataset for association mapping by filtering out SNPs that were not biallelic, had minor allele frequency < 0.01, or were not mapping to the seven *N. crassa* chromosomes. This resulted in 1 473 869 SNPs for the nested association mapping population of 434 strains.

Phenotyping

The association mapping panel strains have been previously phenotyped for growth rate at six different temperatures: 20, 25, 30, 35, 37.5, and 40 $^{\circ}\mathrm{C}$ (Moghadam *et al.*, 2020). Growth rate was measured as the expansion of the mycelium $(\mathrm{mm/h})$ in a linear tube. We used asexual spores to propagate the strains, so the same individuals could be measured multiple times and in different environments. Mean of three replicates was used as the phenotypic value for a given strain in a given temperature. See Moghadam *et al.* (2020) and Kronholm *et al.* (2016) for details about

growth rate measurements.

Statistical analysis

All statistical analyses were performed with the R environment version 3.6.0 (R Core Team, 2019) and the R package 'ggplot2' (Wickham, 2016) was used for plotting. To obtain estimate of the TPC for each strain we fitted a natural spline through the data of each strain, and extracted optimum temperature and maximum growth rate from these fits, see Moghadam *et al.* (2020) for details.

Linkage disequilibrium

To evaluate linkage disequilibrium (LD) between markers in our mapping population, we used only the 118 strains that belong to the natural populations. To evaluate how LD decays over long distance we first sampled 10 000 pairs of SNPs randomly from each chromosome for a total of 70 000 pairwise comparisons, for which we calculated LD. To evaluate LD on finer scales we sampled 10 sets of SNPs spaced evenly across each chromosome. For each set we took the 99 consecutive SNPs from the focal SNP and calculated LD for all unique pairwise comparisons for these 100 SNPs. This resulted in 4950 comparisons for each SNP set, and for 10 sets per chromosome and seven chromosomes this comes to 346 500 comparisons in total.

Coefficient of LD was calculated following Slatkin (2008) as $D = p_{AB} - p_A p_B$, where p_{AB} is the haplotype frequency of haplotype AB and p_A and p_B are allele frequencies for A and B respectively. Then LD was calculated as

$$r^2 = \frac{D^2}{p_A(1-p_A)p_B(1-p_B)}. \tag{1}$$

Genome-wide association

For genome-wide association we used a mixed model association implemented in the GAPIT 3 program (Wang and Zhang, 2021). The model accounts for population structure and relatedness

among individuals (Zhang *et al.*, 2010). The basic model was

$$y = \mathbf{X}\beta + \mathbf{Z}u + e \tag{2}$$

where y is a vector of phenotypic observations, β is a vector of fixed effects including effects of the genetic marker and population structure, u is a vector of random genetic effects for each individual, $\mathbf{X}$ and $\mathbf{Z}$ are design matrices, and e is vector of residual effects. Variance matrix for u is $\sigma_a^2\mathbf{K}$ where σ_a^2 is the additive variance and $\mathbf{K}$ is the kinship matrix. Variance matrix for e is $\sigma_e^2\mathrm{I}$, where σ_e^2 is the residual variance. For population structure correction, a principle component analysis is first done on the SNPs, and the components are used as fixed factors in the model. We chose the first four components for the analysis, as subsequent components explained very little of the variance. When testing for association to TPC breadth, we used growth at either extreme temperature, 20 or 40 $^\circ\mathrm{C}$, and included the maximum growth rate at optimal temperature as an additional covariate to control of variation in TPC elevation.

Testing for association single marker at a time has the disadvantage that nearby causal SNPs cannot be distinguished. It has been shown that testing for association iteratively always conditioning on the most significant marker improves statistical power (Segura *et al.*, 2012). Therefore we used the BLINK method, which is a multilocus method that iteratively alternates between two different models as well as using LD information for the markers (Huang *et al.*, 2018). Simulations have shown that the BLINK method has higher statistical power than single marker methods (Wang and Zhang, 2021; Huang *et al.*, 2018) and it is computationally more efficient than the MLMM method of Segura *et al.* (2012) for large datasets (Wang and Zhang, 2021). Significance threshold for association was set to 0.01 after Bonferroni correction, which corresponds to a p-value of 2.3×10^{-8}.

Allelic effects

For SNPs that were associated with TPC breadth, we examined their allelic effects in subsets of the nested association mapping population. We used a model that included the four principle com-

ponents and maximum growth rate as covariates, effect of temperature, and interaction term with SNP and temperature. The model was:

$$y = \beta_S s + \beta_T z + \beta_M m + \beta_1 p_1 + \beta_2 p_2 + \beta_3 p_3 + \beta_4 p_4 + \beta_I sz + e \tag{3}$$

where β_S is effect of the SNP, β_T effect of temperature, β_M effect of maximum growth rate, $\beta_1 ... \beta_4$ are effects of the population structure principle components, and β_I the effect of interaction between SNP and temperature. We used predicted values to visualize the model results to account for the effects of population structure and the maximum growth rate.

Results

SNP density and linkage disequilibrium

To understand how our SNP density is related to patterns of LD, we evaluated the decay of linkage disequilibrium in our mapping population. First, we sampled pairs of SNPs randomly across all chromosomes to examine how LD decays over long distances across the chromosomes. We observed that on average LD does not persist over megabase scales (Figure S5).

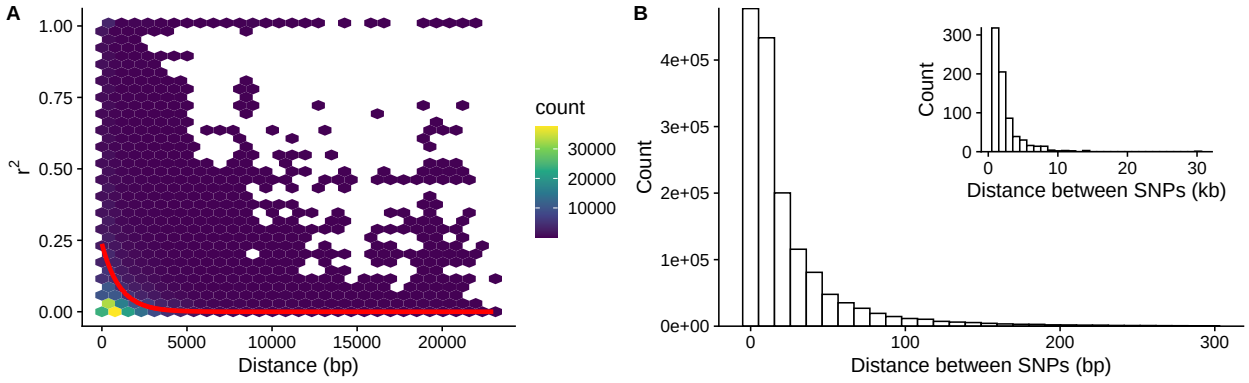

Figure 1: A) Linkage disequilibrium between 346 500 pairwise SNP combinations sampled evenly across the seven chromosomes. Only strains belonging to the set of natural populations are included in the analysis. In the plot data has been binned into hexes. Red line shows exponential decay fit. B) Distribution of physical distance between consecutive SNPs in the natural populations. Inset shows SNPs that are further than 1 kb apart, note the different scales of the two histograms.

Then we examined the decay of LD on a finer scale by sampling sets of consecutive SNPs evenly across the chromosomes. We observed that average LD decayed to very low levels after approximately 2 kb (Figure 1A). However, even if average LD decayed fast, there was large variation in LD, and some SNPs were in high LD over much longer distances (Figure 1A, S5). It is known that there is population structure between the populations from Louisiana and the Caribbean populations (Ellison *et al.*, 2011), so high LD SNPs likely represent SNPs with allele frequency differences between the populations as well as recent mutations where recombination has not had enough time to break down LD.

When we compared the distribution of physical distances between consecutive SNPs we observed that 99% of SNPs are within 215 bp or less of the next SNP (Figure 1B). Only few SNPs had distances longer than 1 kb to the next SNP (Figure 1B), and these were mostly SNPs near the centromeric regions. Since LD decays over longer distances than the SNPs density in our mapping population, we should have a good chance to detect associations, even if our re-sequencing has for some reason missed a causal SNP. Yet, our results suggest that association studies in *N. crassa* need a very dense genotyping to have a chance to detect all causal variants, and long distance haplotype tagging cannot be relied on.

Genome-wide association

When testing for associations at each temperature, we observed 12 associations that were significant after Bonferroni correction at the 0.01 level across all temperatures (Figure 2). We observed both unique associations in a given temperature and associations that were shared across multiple temperatures (Figure 2, Table 2).

There were four missense variants among the significant associations, and the other variants included two synonymous variants, one 3'UTR, three intergenic variants that were close to genes, and one intronic variant (Table 2). If these non-coding variants are true positives, then these are presumably regulatory variants.

One association was shared for 30 and 35 °C in the gene *ncw-1* encoding non-anchored cell

wall protein 1 (Table 2). This was a synonymous variant. There was also a missense variant in the gene *NCU05138*, which is a hypothetical protein, that was associated with growth at 37.5 °C, and which was within 1690 bp of the shared association between 30 and 35 °C (Table 2). This raises the possibility that there is one true association within this region, and these SNPs are in LD with each other.

Table 2: SNPs that were associated with growth. Temp. = Temperature, Chr. = Chromosome. For intergenic SNPs the nearest gene is reported, and distance to the nearest gene is given in the variant column.

Temp. (°C)	Chr.	Position (bp)	p-value	Gene	Annotation	Variant
20	1	7 214 188	6.00×10^{-9}	NCU00775	isocitrate dehydrogenase subunit 1, *tca-6*	intergenic (downstream 156 bp)
25	3	3 119 653	1.31×10^{-10}	NCU00236	flavoprotein oxygenase, *fpo-1*	synonymous
25	5	2 747 660	2.22×10^{-10}	NCU01043	hypothetical protein	3'UTR
25	6	3 669 489	3.27×10^{-12}	NCU17138	haloacid dehalogenase like protein	missense (S/P)
30	3	2 881 603	2.69×10^{-11}	NCU00170	DNAJ domain-containing protein	intergenic (upstream 512 bp)
30	6	3 600 716	1.18×10^{-9}	NCU05137	non-anchored cell wall protein 1, *ncw-1*	synonymous
35	3	2 179 382	9.39×10^{-17}	NCU06278	elongation factor 2, variant 2, *rbg-37*	missense (G/S)
35	6	3 600 716	1.32×10^{-10}	NCU05137	non-anchored cell wall protein 1, *ncw-1*	synonymous
37.5	4	1 399 273	9.52×10^{-10}	NCU07904	short chain dehydrogenase/reductase	intronic, splice polypyrimidine tract
37.5	6	3 599 026	1.20×10^{-9}	NCU05138	glycosyltransferase family 25 protein, *gt25-1*	missense (E/Q)
40	2	3 743 231	1.17×10^{-14}	NCU08705	NACHT domain-containing protein	intergenic (upstream 1182 bp)
40	5	2 708 042	4.85×10^{-9}	NCU01024	MICOS complex subunit MIC12	missense (L/I)

Table 3: SNPs that were associated with TPC shape. Chr. = Chromosome. For intergenic SNPs the nearest gene is reported, and distance to the nearest gene is given in the variant column. For the trait column, Gr(X)$_{\mu max}$ are growth rates at temperature X where maximum growth rate was used as a covariate in the model. Annotations for overlapping genes are separated by "/".

Trait	Chr.	Position (bp)	p-value	Gene	Annotation	Variant
Optimum temp.	6	688 293	9.69×10^{-10}	NCU04755	protein kinase domain-containing protein ppk32, *stk-32*	synonymous
Gr(20 °C)$_{\mu max}$	1	1 638 766	1.92×10^{-9}	NCU02025	Nup53p-like protein	synonymous
Gr(20 °C)$_{\mu max}$	1	1 934 979	5.39×10^{-22}	NCU01940	serine/threonine protein kinase, *ptk-2*	synonymous
Gr(20 °C)$_{\mu max}$	3	2 484 109	1.83×10^{-13}	NCU00064	Protein BNI4	5'UTR
Gr(20 °C)$_{\mu max}$	5	2 439 327	4.42×10^{-9}	NCU03794	periodic tryptophan protein 2	synonymous
Gr(20 °C)$_{\mu max}$	5	2 767 945	2.11×10^{-20}	NCU01049	FAS1 domain-containing protein	intergenic (upstream 352 bp)
Gr(20 °C)$_{\mu max}$	7	720 256	1.47×10^{-17}	NCU06905	tetrahydroxynaphthalene reductase, *tnr-2*	intronic
Gr(20 °C)$_{\mu max}$	7	3 358 427	5.49×10^{-14}	NCU02201 / NCU14149	Laccase for melanin formation-1, *lacm-1* / ncRNA	5'UTR / non-coding transcript variant
Gr(40 °C)$_{\mu max}$	1	6 331 236	2.18×10^{-10}	NCU15038	tRNA-Gly	intergenic (upstream 1420 bp)
Gr(40 °C)$_{\mu max}$	2	3 718 388	5.87×10^{-21}	NCU08696	Ankyrin repeat protein	intergenic (downstream 240 bp)
Gr(40 °C)$_{\mu max}$	3	3 616 832	6.49×10^{-21}	NCU00372	DUF2428 domain-containing protein	intergenic (downstream 952 bp)

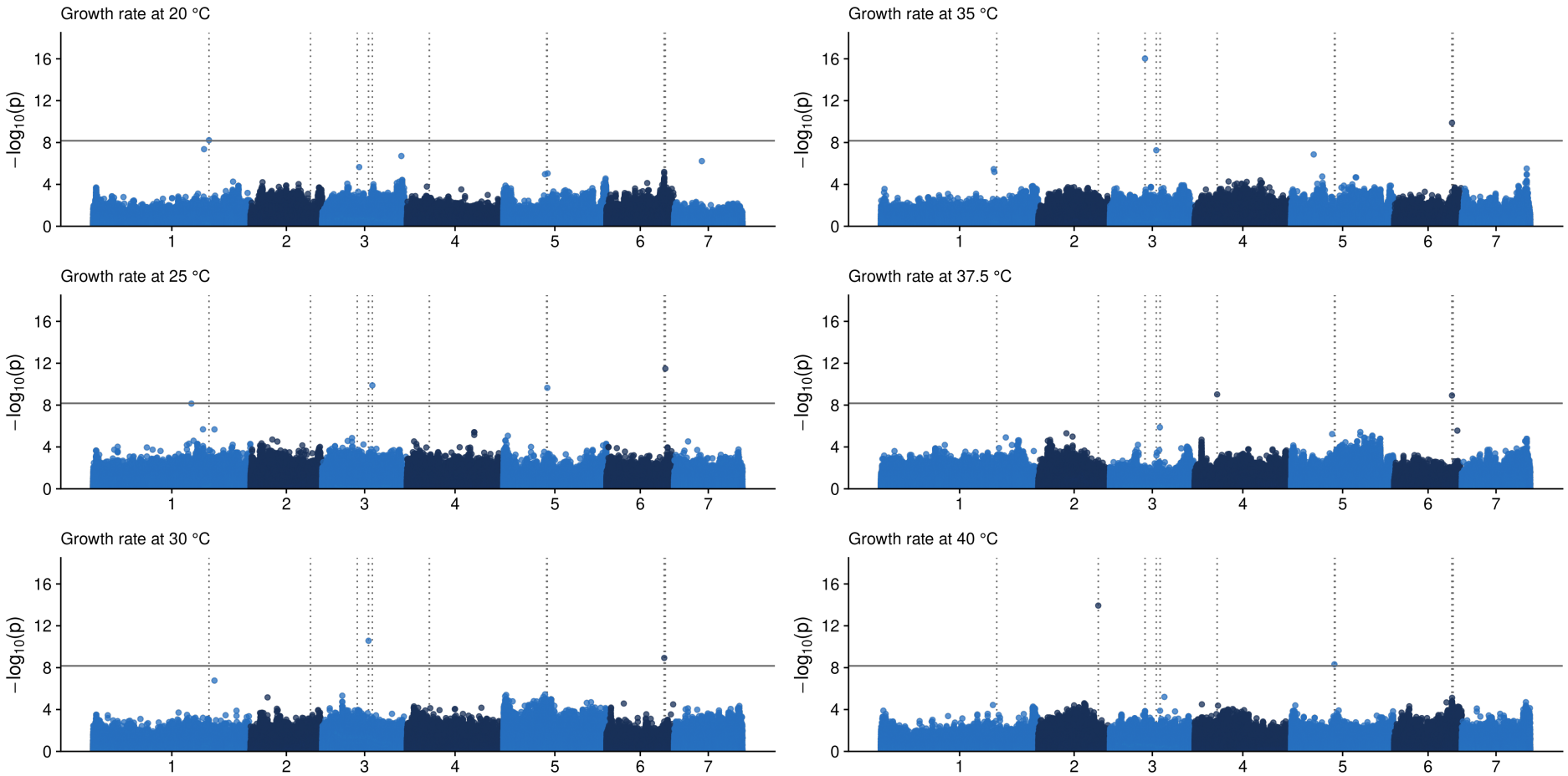

Figure 2: Manhattan plots for growth rate at different temperatures. Solid horizontal line denotes p-value threshold of 0.01 after Bonferroni correction. Dotted vertical lines highlight positions of SNPs that were significant in at least one of the temperatures. Note that because we used a multi marker method to test for associations, we do not expect to see a "skyscraper" of significant SNPs around a significant SNP in the Manhattan plot.

To evaluate whether the associations we observed were true positives, we examined the segregation of associated variants among the strains sampled from natural populations and the different families. In general, we observed that whenever a significant SNP segregated in multiple families its effects were congruent across different families and the natural populations (Figure S6, S7, S8, S9, S10, and S11). In some cases, the directions of the allelic effects on growth rate were the same but the effects were of different magnitude (e.g. Figure S6), one explanation for this is epistasis, so that the magnitude of allelic effects varies in different families because of the genetic background in which they occur. While segregation in different parts of the nested association mapping population does not constitute a validation off the SNPs in an independent set of data, it does seem unlikely that a SNP which shows an effect in the same direction in three different families and in the natural populations, such as the SNP in chromosome 5: 2 708 042 (Figure S11), would be a false positive.

We further tested if we could detect which genes influence thermal performance curve shape, by first approximating the thermal performance curve for each genotype by fitting a spline for growth rate across all measured temperatures. Then we extracted the optimum temperature and the maximum growth rate in this temperature for each genotype. We performed GWAS for optimum temperature to investigate shifts in thermal performance curves, and growth rates for the measured hot and cold extremes that were conditioned on maximum growth rate, by using it as a covariate in the model. This way we can obtain a measure for TPC breadth where the effect of elevation has been removed. Since most variation we observed was for TPC elevation (Moghadam *et al.*, 2020), which may reflect not only temperature specific effects but also effects on growth in general. We observed one significant association for TPC optimum temperature, seven significant associations for growth at 20 °C conditioned on maximum growth rate, and three associations for growth at 40 °C conditioned on maximum growth rate. None of the associations were shared among the three traits (Figure 3).

There was no overlap between significant associations for growth rate at different temperatures and the TPC shape traits (Table 2 and 3). All of the SNPs associated with TPC shape traits were

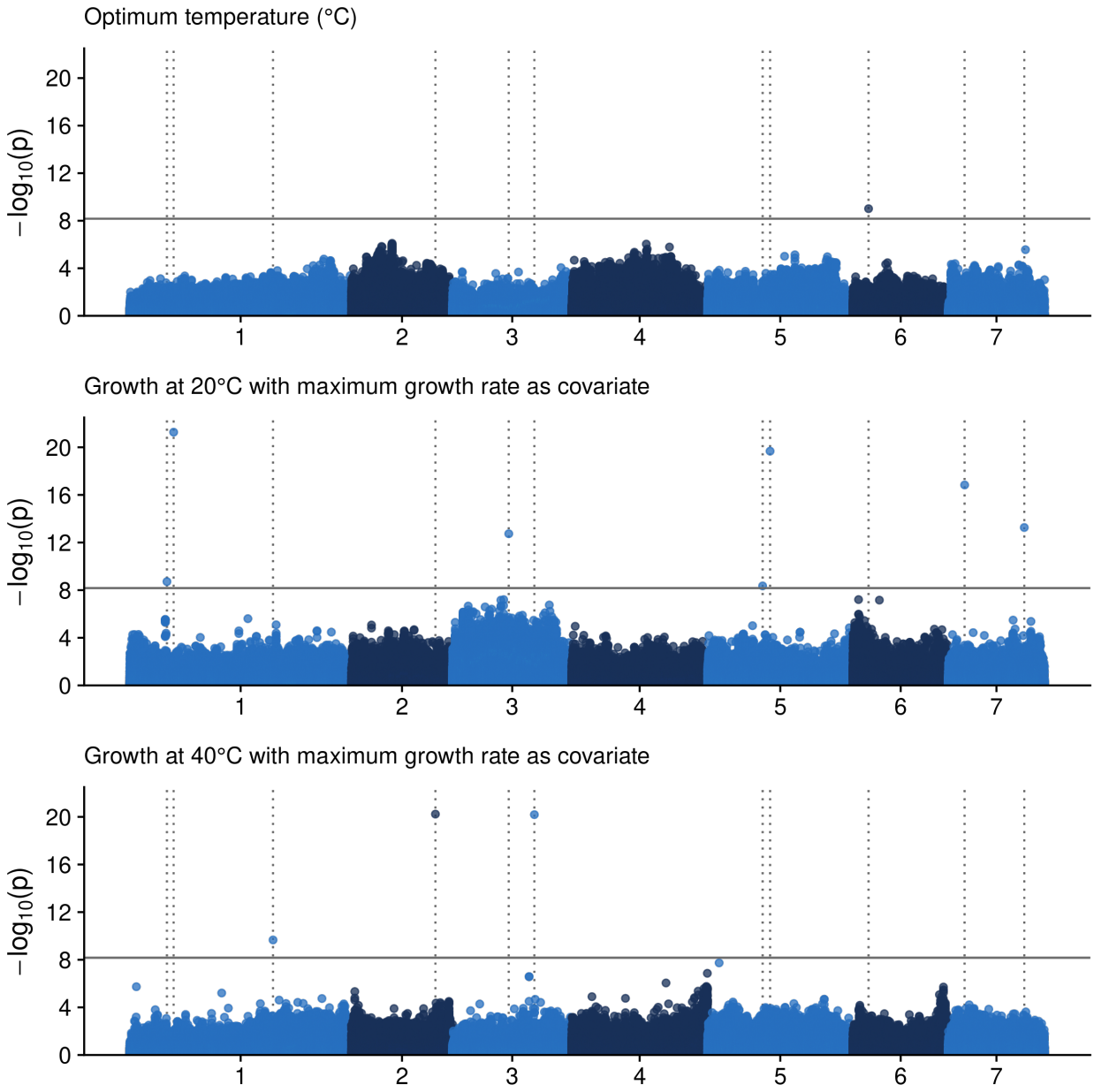

Figure 3: Manhattan plots for thermal performance curve properties. Solid horizontal line denotes p-value threshold of 0.01 after Bonferroni correction. Dotted vertical lines highlight positions of SNPs that were significant for at least one trait.

potential regulatory variants and no missense variants were associated with TPC shape (Table 3). Some of them, such as SNP at 1: 6 331 236 and SNP at 3: 3 616 832 that were associated with growth at 40 °C conditioned for maximum growth rate, were rather far away from the nearest genes (Table 3). Furthermore, the genes they are closest to, a tRNA gene and a hypothetical protein, are not related to temperature in an obvious way.

Allelic effects

When we plotted the allelic effects of all SNPs that had a significant association in one of the temperatures across all temperatures, we observed that in general minor alleles decreased growth (Figure 4). Some SNPs had an effect in only one temperature, such as SNP in chromosome 2: 3 743 231 for which the minor allele decreased growth rate at 40 °C but had no effect in other temperatures (Figure 4). Similarly for SNP in chromosome 5: 2 708 042 for which minor allele decreased growth rate only at 40 °C. Some SNPs had a tendency to have largest effects at either low or high temperatures, such as SNP in chromosome 1: 7 214 188 and SNP in chromosome 6: 3 599 026 (Figure 4). One SNP at chromosome 3: 2 881 603 had the largest effects at the optimal temperature of 35 °C and effects decreased when moving away from the optimum, which suggest the possibility of thermodynamic scaling (Figure 4).

Then we examined the relationship between the size of the allelic effects and minor allele frequencies in the natural populations. We observed a negative relationship between absolute scaled allelic effect and minor allele frequency in the natural populations (Figure 5).

Since we observed that in all significant associations the minor allele decreased growth, and that allelic effects get smaller as allele frequency increases in the natural populations, these associated alleles are likely mildly deleterious alleles segregating at low frequencies in the natural populations.

Then we examined allelic effects of SNPs that were associated with growth at either 20 or 40 °C when maximum growth rate was used a covariate. Since the effect of variation in elevation should be removed from this data, we were interested were there any trade-offs between the temperatures. That is, did the allelic effect switch its sign, regardless of their genome wide significance. Out of

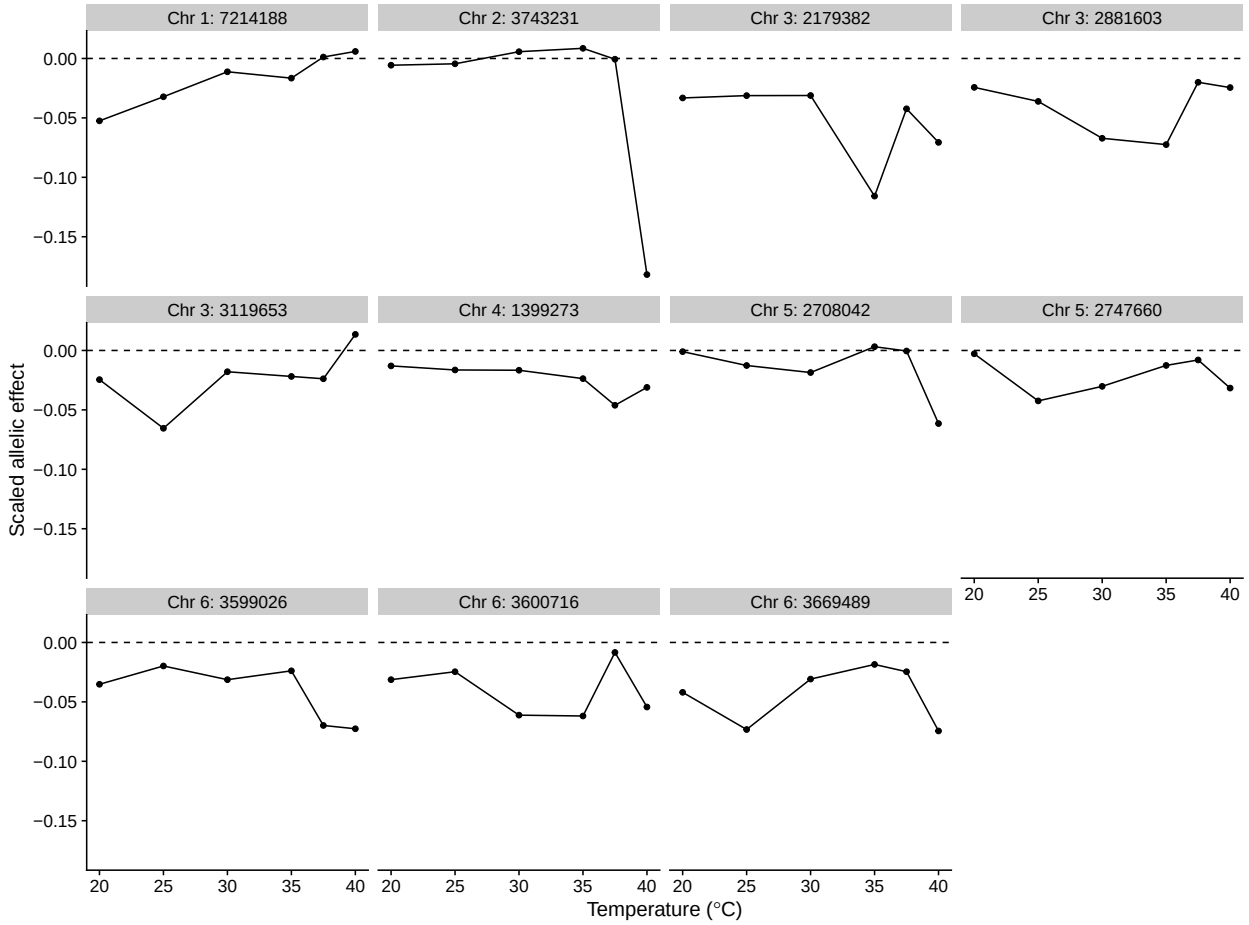

Figure 4: Scaled allelic effects of SNPs that were associated with growth at any temperature over all of the measured temperatures. Allelic effects are reported relative to the major allele, that is if the minor allele decreases growth rate allelic effect has a negative sign.

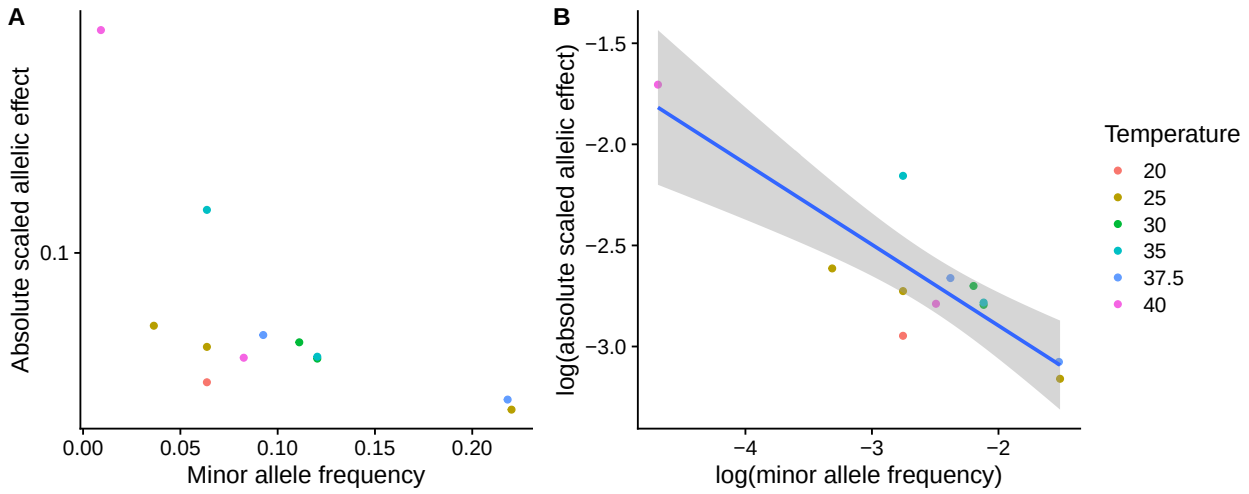

Figure 5: A) Absolute scaled allelic effects of associated SNPs plotted against minor allele frequency in natural populations. Minor allele frequencies are frequencies among the strains from the natural populations, not in the whole nested association mapping population. B) The same data in a log-log plot, allelic effects get smaller as minor allele frequency increases.

the ten SNP that were significantly associated TPC breadth in either direction, we observed some indications of trade-offs for five of them (Figure 6).

Three SNPs in chromosome 1 displayed a potential trade-off. There was a trade-off for SNP in chromosome 1 at position 1 638 766 among the family G strains. Effect of SNP at 20 °C was -0.39, $p = 0.01$, and the effect at 40 °C was 0.79, and the interaction term had a $p = 1.68 \times 10^{-11}$. However, no trade-off was observed among strains belonging to family C or among the strains from natural populations, where this SNP also segragated. There was also a nearby SNP in chromosome 1 at position 1 934 979 where a trade-off was also observed among strains of family G, the effect of the SNP at 20 °C was -0.43, $p = 0.01$, and the effect of the SNP at 40 °C was 0.77, and $p = 3.20 \times 10^{-12}$ for the interaction term. But this tradeoff was not observed among the natural strains, where the SNP had an effect only at 20 °C (Figure 6). These two SNPs are close together physically, and within family G, these effects are likely similar due to linkage. So we cannot be certain which of these SNPs is causally behind the trade-off, or whether the observed trade-off in family G is the joint effect of multiple linked loci. We also observed that for a SNP in chromosome 1 at position 6 331 236 estimates of allelic effects had opposite signs for family G, but the effect of SNP was not significant at 20 °C, $p = 0.33$ even if the interaction term was

significant, $p = 8.59 \times 10^{-15}$. We could not assess this potential trade-off in other parts of the nested association mapping population, since this SNP is carried only by strain 851, which is one of the parents of family G. For these three SNPs the trade-off is present potentially only in family G and we could not confirm it in any other part of the mapping population. Therefore, we view the evidence for trade-offs as weak for the these SNPs.

Another two SNPs in chromosome 7 also showed a potential trade-off. For the SNP in chromosome 7 at position 720 256 among family D had opposite signs for allelic effects: -0.23 at 20 °C, $p = 0.11$ and 0.15 at 40 °C, $p = 0.0003$ for the interaction term. Since the main effect of the SNP was not significant this remains only suggestive. However, for the natural strains the estimate of SNP effect at 20 °C was -0.13, $p = 0.02$ and effect at 40 °C was 0.19, and $p = 0.0001$ for the interaction term. So, a significant trade-off was present among the natural strains for this SNP, and the effects go in the same direction in family D. The second SNP in chromosome 7 at position 3 358 427 had a significant trade-off among the natural strains. The effect of the SNP at 20 °C was 0.12, $p = 0.003$ and the effect at 40 °C was -0.14, $p = 0.03$ for the interaction term. Observing a significant trade-off for the natural populations seems stronger evidence than just for a single family.

The other SNPs did not have significant trade-offs, either allelic effects went generally in the same direction for both temperatures, but the effect for the other temperature was weak enough so that these did not come up at genome wide significance level for both temperatures, or that there was an effect only in the other temperature (Figure S12).

Discussion

While association mapping has been previously used in *N. crassa* to discover genes affecting quantitative traits (Palma-Guerrero *et al.*, 2013), our results demonstrate that our nested association mapping population can successfully used to map loci underlying quantitative traits. As the strains can be stored in the freezer, this population can be used again for other traits. In the future statis-

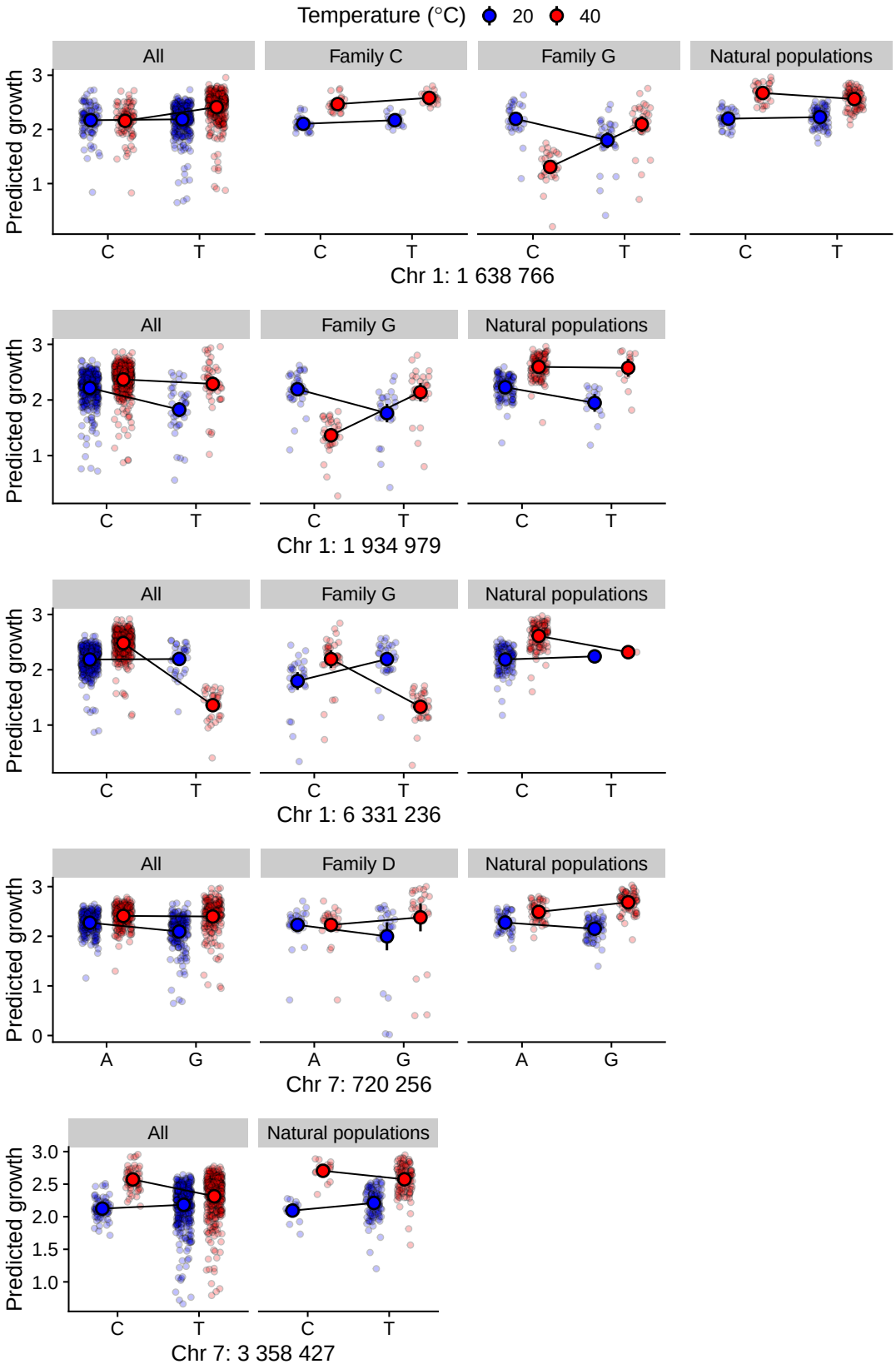

Figure 6: Allelic effects of SNPs associated with TPC breadth, which show potential trade-offs between 20 and 40 °C. Y-axis shows model predictions.

tical power could be improved by making more crosses using more parents so that singleton SNPs among the natural strains will be segregating in multiple families. This would also improve the estimation of allelic effects if the alleles occur in multiple backgrounds.

Our results allow some insight into the identity of the loci that influence growth at different temperatures and the functions of those loci. Many of the genes associated with growth at different temperatures seem to be genes important for growth rather than a temperature response itself. For example, the gene *tca-6* associated at 20 °C functions in the tricarboxylic acid cycle to release energy from stored nutrients. The gene *fpo-1* associated at 25 °C encodes for flavoprotein oxygenase, which belongs to a class of enzymes that function, e.g., in energy production, degradation of organic material, biosynthesis of primary metabolites like pigments (Kerschbaumer *et al.*, 2022), and amino acid metabolism (Huberman *et al.*, 2021), and deletion mutants of *fpo-1* gene have been shown to suffer from reduced reproductive ability (Lan *et al.*, 2021). Moreover, the gene *ncw-1* associated in both 30 and 35 °C which is known to function in carbohydrate metabolic process, as its deletion promotes cellulase production by increasing cellobiose uptake in *N. crassa* through transporter expression (Lin *et al.*, 2017).

We did observe one locus that has a clear link to temperature response. The gene *NCU00170* associated at 30 °C encodes DnaJ domain-containing protein. DnaJ is an important molecular chaperone and a member of the Hsp40 family, which regulates the activity of Hsp70s and fungal ATPase machinery (Roy and Tamuli, 2022). Heat shock proteins (Hsps) are involved in a wide array of biological processes in fungi, including growth, development, and general stress resistance (Abu Bakar *et al.*, 2020). In *Neurospora*, DnaJs are the largest class of Hsps, proteins which are produced to prevent protein unfolding and denaturation under sub-optimal or stressful conditions (Borkovich *et al.*, 2004; Kapoor and Roy, 2014).

Further genes were also related to growth. We found that a missense SNP in the gene *rbg-37* was associated at 35 °C, this gene encodes a variant elongation factor 2. This protein binds the ribosomal subunits together into a ribosome and functions in the chain elongation during protein synthesis. Previously the gene *cot-3* encoding translation elongation factor 2 has been found to be

involved in hyphal growth at elevated temperatures in *N. crassa* (Propheta *et al.*, 2001). We also found a missense SNP associated with growth at 37.5 °C in the gene *gt25-1* encoding glycosyltransferase family 25 protein, glycosyltransferases have been linked to fungal hyphal growth on solid matrices (King *et al.*, 2017). Finally, a missense SNP the gene *NCU01024* was associated at 40 °C, this gene encodes the MICOS complex subunit MIC12, which is part of the mitochondrial inner membrane.

For the TPC shape traits, we observed one association with the TPC optimum temperature itself, for the gene *stk-32*, which encodes a protein kinase. In filamentous fungi this gene has been linked to the regulatory mechanism of mycelial growth under heat stress (Yang *et al.*, 2022), and the deletion mutants of the *stk-32* gene in *N. crassa* have reduced hyphal growth (Park *et al.*, 2011).

When we tested for associations for TPC breadth, by using the maximal growth rate as a covariate so the effect of elevation variation should be removed, we observed that many of these genes had growth and cell wall related functions. At 20 °C genes associated with growth when controlling for maximal growth rate included *ptk-2* a protein kinase that in *N. crassa* is involved in the hyphal tip-growing which relies upon a turgor maintained by accumulation of osmotically active solutes and ion uptake (Lew and Kapishon, 2009). As well as the gene *NCU00064* which encodes the BNI4 protein that in *N. crassa*, affects the cell wall building and hyphal growth (Verdín *et al.*, 2019). We observed an association in the gene *rbg-11*, which encodes periodic tryptophan protein 2 homolog that affects cell polarity and growth. In yeast, this protein is involved in ribosome biogenesis and regulation of the cell cycle (Neer *et al.*, 1994). Another associated gene was *NCU01049*, which encodes FAS1 domain-containing protein. Fatty acid synthase beta subunit dehydratse (FAS1) belongs to conserved fasciclin 1 domain, that functions in fatty acid and lipid biosynthesis. Also, the lipid biosynthesis produces glycerol, which is important in fueling the turgor pressure necessary for germination and penetration of plant host by fungi (Sangappillai and Nadarajah, 2020).

In addition to these genes involved in growth processes, we found two genes involved in melanin biosynthesis to be associated with TPC breadth. The gene *tnr-2* encodes a tetrahydroxynaphthalene reductase, which is an enzyme that functions in the fungal biosynthesis of melanin. Melanin

strengthens the cell wall and is important for adaptation to stressful conditions (Suthar *et al.*, 2023). The other gene involved in melanin production was *lacm-1*. This gene encodes an enzyme that catalyzes melanin formation for making strong cell wall structure, also in perithecium and ascospores (Ao *et al.*, 2019). Furthermore, this gene overlaps with a non-coding RNA gene *NCU14149*, but no obvious function can be assigned to this ncRNA.

For genes associated with TPC breadth in 40 °C, the gene *NCU15038* encodes a glycine transfer RNA. Glycine transfer RNA can modify fungal cell walls and membrane constituents by adding amino acids to them (Grob *et al.*, 2022). Another associated gene was *NCU08696*, which encodes an ankyrin repeat protein that functions in ion transmembrane transporter activity and protein–protein interactions involved in the formation of transcription complexes. Mutations in genes that encode ankyrin-like proteins can cause defects in gene expression, and it has been linked to mycelial growth in fungi (Situ *et al.*, 2023). The final associated gene *NCU00372*, was a DUF2428 domain-containing protein, this protein is highly conserved and known to be required for tRNA methylation in yeasts and interestingly, is in general involved in energy metabolism and growth response during cold conditions (Dong *et al.*, 2019).

We know that majority of genetic variation in growth at different temperatures is variation in TPC elevation (Moghadam *et al.*, 2020). When we tested for associations at specific temperatures, we observed both unique associations at specific temperatures, but also associations that were shared across multiple temperatures. Growth in nearby temperatures has a positive and high genetic correlation (Moghadam *et al.*, 2020), so shared associations are expected. It is perhaps surprising that so few shared associations were detected. Since we can only detect associations with high and moderate effects, it may be that alleles that affect growth at multiple temperatures have smaller effects in general and we miss many of the shared associations. Moreover, we did not observe strong evidence of thermodynamic scaling for allelic efffects, we observed only one locus for which allelic effects were compatible thermodynamic scaling. While there is a correlation between optimum temperature and maximum growth rate at the phenotypic level (Moghadam *et al.*, 2020), it seems that allelic effects do not often scale this way. Rather allelic effects tend to be limited for

435 certain temperature ranges.

436 For growth at specific temperatures we observed that effects of the minor allele had a negative
437 correlation with minor allele frequency in the natural populations. This suggests that alleles with
438 large effects on growth are mostly deleterious, and are being kept at low frequencies by negative
439 selection (Barton and Keightley, 2002; Keightley and Lynch, 2003).

440 Allelic variation with antagonistic pleiotropy can lead to divergent adaptation when certain
441 alleles act to increase fitness in one environment and conversely decrease in others, which is a pre-
442 requisite for trade-offs in TPCs (Angilletta *et al.*, 2003; Yamahira *et al.*, 2007; Berger *et al.*, 2013;
443 Murren *et al.*, 2015). In a study of hot and cold adapted experimental lines of dung fly (*Sepsis*
444 *punctum*), temperature-specific allelic effects on growth rate were found after 20 generations, but no
445 trade-offs in TPC shape were observed (Berger *et al.*, 2014). Another study with European grayling
446 (*Thymallus thymallus*) adapted to differing thermal environments demonstrated temperature-driven
447 gene expression changes constrained by the level of gene pleiotropy (Papakostas *et al.*, 2014). In-
448 terestingly, they found that genes with low pleiotropy levels were the main drivers of the changes in
449 gene expression, whereas highly pleiotropic genes had limited expression response to temperature
450 treatment.

451 Antagonistic pleiotropy can be produced for example by alleles that encode different enzyme
452 variants acting differently across temperatures (Huey and Kingsolver, 1989). However, typically the
453 genetic variance for temperature specificity of enzymatic reactions is low (Hochachka and Somero,
454 2002; Latimer *et al.*, 2014). Other possible mechanisms are the frequency change at loci affecting
455 overall performance but with differing strength between temperatures, and the difference in the
456 magnitude of the allelic effects, for example, between cold and hot temperatures (Latimer *et al.*,
457 2015).

458 We only detected weak evidence for trade-offs out of the ten SNPs associated with TPC breadth
459 in either hot or cold temperatures, potential trade-off were detected for five SNPs, and for three of
460 those evidence of trade-off came from a single family, and the trade-off was not supported by the
461 strains from natural populations. It may be that there is a modifier locus present in this family,

that is an epistatic effect, or that effects of multiple loci that affect growth only in hot or cold temperature are joined together due to linkage and appear as a trade-off. Either way, evidence of trade-off seems relatively weak for these three SNPs. For the two remaining SNPs evidence of trade-off was stronger, since the trade-off was observed among the natural populations.

Since we know that at the phenotypic level this hot-cold trade-off represents a minor aspect of the genetic variation (Moghadam *et al.*, 2020), it is not that surprising that that only few loci display evidence of trade-offs. Our results highlight the need to reconsider some aspects of theories related to TPC evolution, where antagonistic pleiotropy is predicted to have an important role in maintaining variation in TPCs (Lynch and Gabriel, 1987; Gilchrist, 1995). Our results suggest that Some trade-offs at the allelic level exist, but it seems that in majority of cases alleles have temperature specific effects. Our results are in line with a genome-wide study of thermal tolerance in *Drosophila melanogaster*, while some genes showed pleiotropic effects shaping tolerance at upper and lower thermal limits (Lecheta *et al.*, 2020). The heat and cold tolerance had no overlapping SNPs, so distinct molecular processes evolving indepently in response to changing environmental conditions are more likely.

Conclusion

In summary, we identified that many loci contributing to TPC variation are loci that may affect growth and metabolism in general, as well as the fungal cell wall. Finding genes related to growth is understandable, since most of this variation is related to TPC elevation, but the associated loci have temperature specific alleles. We did detect some loci that had been previously linked with temperature stress or stress response in general. We also found that trade-offs between hot and cold temperatures do exist at the allelic level, but they are a minor part of the overall variation. Therefore, variation in TPCs is unlikely to be driven solely by trade-offs.

Data access

The genome sequencing data generated in this project has been deposited to sequence read archive under accession number XXXXX-XXXX. RAD sequencing data has been deposited under accession number XXXX-XXXX. Genotyping information and related cripts for the nested association mapping population can be accessed at yyyy.doi. Phenotypes and analysis scripts can be accessed at yyyy.doi.

Acknowledgements

The authors wish to acknowledge CSC – IT Center for Science, Finland, for computational resources, and the Fungal Genetics Stock Center for the strains used in this study. This study was funded by grants from Emil Aaltonen foundation to IK and ER, University of Jyväskylä Doctoral Programme in Biological and Environmental Science to ER, Ella & Georg Ehrnrooth foundation to IK, and Academy of Finland Research Fellowships to IK (no. 321584) and TK (no. 278751).

Author contributions

The study was conceived by I.K., T.K, and E.R. Experiments were performed by N.N.M., H.-R.L., K.S., P.A.M.S., E.R. and I.K. Data was analyzed by I.K. and E.R., I.K. and E.R. wrote the manuscript. All authors edited the final manuscript.

References

Abu Bakar N, Karsani SA, Alias SA (2020). Fungal survival under temperature stress: a proteomic perspective. *PeerJ* **8**: e10423.

Angilletta MJ, Huey RB, Frazier MR (2010). Thermodynamic effects on organismal performance: Is hotter better? *Physiological and Biochemical Zoology* **83**: 197–206. PMID: 20001251. **URL:** *https://doi.org/10.1086/648567*

Angilletta MJ, Wilson RS, Navas CA, James RS (2003). Tradeoffs and the evolution of thermal reaction norms. *Trends in Ecology & Evolution* **18**: 234 – 240. **URL:** *http://www.sciencedirect.com/science/article/pii/S0169534703000879*

Angilletta Jr MJ (2009). *Thermal Adaptation: A Theoretical and Empirical Synthesis*. Oxford University Press. **URL:** *https://doi.org/10.1093/acprof:oso/9780198570875.001.1*

Ao J, Bandyopadhyay S, Free SJ (2019). Characterization of the *Neurospora crassa* DHN melanin biosynthetic pathway in developing ascospores and peridium cells. *Fungal Biology* **123**: 1–9. **URL:** *https://www.sciencedirect.com/science/article/pii/S1878614618303519*

Araújo MB, Ferri-Yáñez F, Bozinovic F, Marquet PA, Valladares F, Chown SL (2013). Heat freezes niche evolution. *Ecology Letters* **16**: 1206–1219. **URL:** *http://dx.doi.org/10.1111/ele.12155*

Arcus VL, Prentice EJ, Hobbs JK, Mulholland AJ, Van der Kamp MW, Pudney CR, *et al.* (2016). On the temperature dependence of enzyme-catalyzed rates. *Biochemistry* **55**: 1681–1688. **URL:** *https://doi.org/10.1021/acs.biochem.5b01094*

Asbury D, Angilletta Jr M (2010). Thermodynamic effects on the evolution of performance curves. *The American Naturalist* **176**: E40–E49. PMID: 20528470. **URL:** *https://doi.org/10.1086/653659*

Baird NA, Etter PD, Atwood TS, Currey MC, Shiver AL, Lewis ZA, *et al.* (2008). Rapid snp discovery and genetic mapping using sequenced rad markers. *PLoS ONE* **3**: e3376.

Bartheld JL, Artacho P, Bacigalupe L (2017). Thermal performance curves under daily thermal fluctuation: A study in helmeted water toad tadpoles. *Journal of Thermal Biology* **70**: 80–85. **URL:** *https://linkinghub.elsevier.com/retrieve/pii/S0306456517300244*

Barton NH, Keightley PD (2002). Understanding quantitative genetic variation. *Nature Reviews Genetics* **3**: 11–21. 1471-0056 10.1038/nrg700 10.1038/nrg700. **URL:** *http://dx.doi.org/10.1038/nrg700*

Berger D, Postma E, Blanckenhorn WU, Walters RJ (2013). Quantitative genetic divergence and standing genetic (co)variance in thermal reaction norms along latitude. *Evolution* **67**: 2385–2399. **URL:** *https://onlinelibrary.wiley.com/doi/abs/10.1111/evo.12138*

Berger D, Walters RJ, Blanckenhorn WU (2014). Experimental evolution for generalists and specialists reveals multivariate genetic constraints on thermal reaction norms. *Journal of Evolutionary Biology* **27**: 1975–1989. **URL:** *https://doi.org/10.1111/jeb.12452*

Borkovich KA, Alex LA, Yarden O, Freitag M, Turner GE, Read ND, *et al.* (2004). Lessons from the genome sequence of neurospora crassa: Tracing the path from genomic blueprint to multicellular organism. *Microbiology and Molecular Biology Reviews* **68**: 1–108. **URL:** *http://mmbr.asm.org/content/68/1/1.abstract*

Catchen JM, Amores A, Hohenlohe P, Cresko W, Postlethwait JH (2011). Stacks: Building and genotyping loci *de novo* from short-read sequences. *G3: Genes, Genomes, Genetics* **1**: 171–182. **URL:** *https://www.g3journal.org/content/1/3/171*

Deutsch CA, Tewksbury JJ, Huey RB, Sheldon KS, Ghalambor CK, Haak DC, *et al.* (2008). Impacts of climate warming on terrestrial ectotherms across latitude. *Proceedings of the National Academy of Sciences* **105**: 6668–6672. **URL:** *http://www.pnas.org/content/105/18/6668.abstract*

Dillon ME, Wang G, Huey RB (2010). Global metabolic impacts of recent climate warming. *Nature* **467**: 704–706. **URL:** *https://doi.org/10.1038/nature09407*

Dong Y, Teleman AA, Jedmowski C, Wirtz M, Hell R (2019). The *Arabidopsis* THADA homologue modulates TOR activity and cold acclimation. *Plant Biology* **21**: 77–83. **URL:** *https://onlinelibrary.wiley.com/doi/abs/10.1111/plb.12893*

Ellison CE, Hall C, Kowbel D, Welch J, Brem RB, Glass NL, *et al.* (2011). Population genomics and local adaptation in wild isolates of a model microbial eukaryote. *Proceedings of the National Academy of Sciences* **108**: 2831–2836.

Frazier MR, Huey RB, Berrigan D (2006). Thermodynamics constrains the evolution of insect population growth rates: "warmer is better.". *The American Naturalist* **168**: 512–520. PMID: 17004222. **URL:** *https://doi.org/10.1086/506977*

Gilchrist GW (1995). Specialists and generalists in changing environments. i. fitness landscapes of thermal sensitivity. *The American Naturalist* **146**: 252–270.

Grob G, Hemmerle M, Yakobov N, Mahmoudi N, Fischer F, Senger B, *et al.* (2022). tRNA-dependent addition of amino acids to cell wall and membrane components. *Biochimie* **203**: 93–105. Tailored Lipids: from synthesis to specific biological functions. **URL:** *https://www.sciencedirect.com/science/article/pii/S030090842200253X*

Hochachka PW, Somero GN (2002). *Biochemical adaptation*. Oxford University Press, Inc., New York.

Huang M, Liu X, Zhou Y, Summers RM, Zhang Z (2018). BLINK: a package for the next level of genome-wide association studies with both individuals and markers in the millions. *GigaScience* **8**: giy154. **URL:** *https://doi.org/10.1093/gigascience/giy154*

Huberman LB, Wu VW, Kowbel DJ, Lee J, Daum C, Grigoriev IV, *et al.* (2021). DNA affinity purification sequencing and transcriptional profiling reveal new aspects of nitrogen regulation in a filamentous fungus. *Proceedings of the National Academy of Sciences* **118**: e2009501118. **URL:** *https://www.pnas.org/doi/abs/10.1073/pnas.2009501118*

Huey RB, Kingsolver JG (1989). Evolution of thermal sensitivity of ectotherm performance. *Trends in Ecology & Evolution* **4**: 131 – 135. **URL:** *http://www.sciencedirect.com/science/article/pii/0169534789902115*

Huey RB, Kingsolver JG (1993). Evolution of resistance to high temperature in ectotherms. *The American Naturalist* **142**: S21–S46. **URL:** *http://www.jstor.org/stable/2462707*

IPCC (2013). *Summary for Policymakers*, Cambridge University Press, Cambridge, United Kingdom and New York, NY, USA, book section SPM, p. 1–30. **URL:** *www.climatechange2013.org*

Kapoor M, Roy SS (2014). A bird's eye view of molecular chaperones and some facets of the heat shock response of neurospora crassa. In: Chakraborty BN, Chakraborty U (eds.), *Review of Plant Pathology*, Scientific Publishers (India), Jothpur, vol. 6, pp. 1–57.

Keightley PD, Lynch M (2003). Toward a realistic model of mutations affecting fitness. *Evolution* **57**: 683–685.

Kelleher J, Ness RW, Halligan DL (2013). Processing genome scale tabular data with wormtable. *BMC Bioinformatics* **14**: 1–5. **URL:** *http://dx.doi.org/10.1186/1471-2105-14-356*

Kerschbaumer B, Bijelic A, Macheroux P (2022). Flavofun: Exploration of fungal flavoproteomes. *Frontiers in Catalysis* **2**: 1021691.

King R, Urban M, Lauder RP, Hawkins N, Evans M, Plummer A, *et al.* (2017). A conserved fungal glycosyltransferase facilitates pathogenesis of plants by enabling hyphal growth on solid surfaces. *PLoS pathogens* **13**: e1006672.

Klepsatel P, Gáliková M, De Maio N, Huber CD, Schlötterer C, Flatt T (2013). Variation in thermal performance and reaction norms among populations of *Drosophila melanogaster*. *Evolution* **67**: 3573–3587. **URL:** *https://onlinelibrary.wiley.com/doi/abs/10.1111/evo.12221*

Kontopoulos DG, van Sebille E, Lange M, Yvon-Durocher G, Barraclough TG, Pawar S (2020). Phytoplankton thermal responses adapt in the absence of hard thermodynamic constraints. *Evolution* **74**: 775–790. **URL:** *https://onlinelibrary.wiley.com/doi/abs/10.1111/evo.13946*

Krenek S, Berendonk TU, Petzoldt T (2011). Thermal performance curves of *Paramecium caudatum*: A model selection approach. *European Journal of Protistology* **47**: 124 – 137. **URL:** *http://www.sciencedirect.com/science/article/pii/S0932473910000878*

Kronholm I, Bassett A, Baulcombe D, Collins S (2017). Epigenetic and genetic contributions to adaptation in *Chlamydomonas*. *Molecular Biology and Evolution* **34**: 2285–2306. **URL:** + *http://dx.doi.org/10.1093/molbev/msx166*

Kronholm I, Johannesson H, Ketola T (2016). Epigenetic control of phenotypic plasticity in the filamentous fungus *Neurospora crassa*. *G3: Genes|Genomes|Genetics* **6**: 4009–4022. **URL:** *http://www.g3journal.org/content/early/2016/09/29/g3.116.033860.abstract*

Lan N, Ye S, Hu C, Chen Z, Huang J, Xue W, *et al.* (2021). Coordinated regulation of protoperithecium development by MAP kinases MAK-1 and MAK-2 in *Neurospora crassa*. *Frontiers in Microbiology* **12**: 769615.

Latimer CAL, Foley BR, Chenoweth SF (2015). Connecting thermal performance curve variation to the genotype: a multivariate QTL approach. *Journal of Evolutionary Biology* **28**: 155–168. **URL:** *https://onlinelibrary.wiley.com/doi/abs/10.1111/jeb.12552*

Latimer CAL, McGuigan K, Wilson RS, Blows MW, Chenoweth SF (2014). The contribution of spontaneous mutations to thermal sensitivity curve variation in *Drosophila serrata*. *Evolution* **68**: 1824–1837. **URL:** *https://onlinelibrary.wiley.com/doi/abs/10.1111/evo.12392*

Lecheta MC, Awde DN, O'Leary TS, Unfried LN, Jacobs NA, Whitlock MH, *et al.* (2020). Integrating GWAS and transcriptomics to identify the molecular underpinnings of thermal stress responses in *Drosophila melanogaster*. *Frontiers in genetics* **11**: 658.

Lew RR, Kapishon V (2009). Ptk2 contributes to osmoadaptation in the filamentous fungus *Neurospora crassa*. *Fungal Genetics and Biology* **46**: 949–955.

Li H (2013). Aligning sequence reads, clone sequences and assembly contigs with BWA-MEM. *arXiv:13033997 [q-bioGN]* .

Lin L, Chen Y, Li J, Wang S, Sun W, Tian C (2017). Disruption of non-anchored cell wall protein NCW-1 promotes cellulase production by increasing cellobiose uptake in *Neurospora crassa*. *Biotechnology letters* **39**: 545–551.

Logan ML, Curlis JD, Gilbert AL, Miles DB, Chung AK, McGlothlin JW, *et al.* (2018). Thermal physiology and thermoregulatory behaviour exhibit low heritability despite genetic diver-

gence between lizard populations. *Proceedings of the Royal Society B: Biological Sciences* **285**: 20180697. **URL:** *https://royalsocietypublishing.org/doi/abs/10.1098/rspb.2018.0697*

Logan ML, Minnaar IA, Keegan KM, Clusella-Trullas S (2020). The evolutionary potential of an insect invader under climate change. *Evolution* **74**: 132–144. **URL:** *https://onlinelibrary.wiley.com/doi/abs/10.1111/evo.13862*

Lynch M, Gabriel W (1987). Environmental tolerance. *The American Naturalist* **129**: 283–303.

Maclean HJ, Sørensen JG, Kristensen TN, Loeschke V, Beedholm K, Kellermann V, *et al.* (2019). Evolution and plasticity of thermal performance: an analysis of variation in thermal tolerance and fitness in 22 drosophila species. *Phil Trans R Soc B* **374**: 20180548.

Malusare SP, Zilio G, Fronhofer EA (2023). Evolution of thermal performance curves: A meta-analysis of selection experiments. *Journal of Evolutionary Biology* **36**: 15–28. **URL:** *https://onlinelibrary.wiley.com/doi/abs/10.1111/jeb.14087*

Martins F, Kruuk L, Llewelyn J, Moritz C, Phillips B (2019). Heritability of climate-relevant traits in a rainforest skink. *Heredity* **122**: 41–52. **URL:** *https://doi.org/10.1038/s41437-018-0085-y*

McKenna A, Hanna M, Banks E, Sivachenko A, Cibulskis K, Kernytsky A, *et al.* (2010). The Genome Analysis Toolkit: a MapReduce framework for analyzing next-generation DNA sequencing data. *Genome Research* **20**: 1297–1303. **URL:** *http://dx.doi.org/10.1101/gr.107524.110*

Merilä J, Hendry AP (2014). Climate change, adaptation, and phenotypic plasticity: the problem and the evidence. *Evol Appl* **7**: 1–14. **URL:** *http://dx.doi.org/10.1111/eva.12137*

Moghadam NN, Sidhu K, Summanen PAM, Ketola T, Kronholm I (2020). Quantitative genetics of temperature performance curves of *Neurospora crassa*. *Evolution* **74**: 1772–1787. **URL:** *https://onlinelibrary.wiley.com/doi/abs/10.1111/evo.14016*

Murren CJ, Auld JR, Callahan H, Ghalambor CK, Handelsman CA, Heskel MA, *et al.* (2015). Constraints on the evolution of phenotypic plasticity: limits and costs of phenotype and plasticity. *Heredity* **115**: 293–301.

Neer EJ, Schmidt CJ, Nambudripad R, Smith TF (1994). The ancient regulatory-protein family of WD-repeat proteins. *Nature* **371**: 297–300.

Palma-Guerrero J, Hall CR, Kowbel D, Welch J, Taylor JW, Brem RB, *et al.* (2013). Genome wide association identifies novel loci involved in fungal communication. *PLoS Genetics* **9**: e1003669.

Papakostas S, Vøllestad LA, Bruneaux M, Aykanat T, Vanoverbeke J, Ning M, *et al.* (2014). Gene pleiotropy constrains gene expression changes in fish adapted to different thermal conditions. *Nature Communications* **5**: 4071.

Park G, Servin JA, Turner GE, Altamirano L, Colot HV, Collopy P, *et al.* (2011). Global analysis of serine-threonine protein kinase genes in *Neurospora crassa*. *Eukaryotic cell* **10**: 1553–1564.

Propheta O, Vierula J, Toporowski P, Gorovits R, Yarden O (2001). The *Neurospora crassa* colonial temperature-sensitive 3 (*cot-3*) gene encodes protein elongation factor 2. *Molecular Genetics and Genomics* **264**: 894–901.

Querns A, Wooliver R, Vallejo-Marín M, Sheth SN (2022). The evolution of thermal performance in native and invasive populations of *Mimulus guttatus*. *Evolution Letters* **6**: 136–148. **URL:** *https://onlinelibrary.wiley.com/doi/abs/10.1002/evl3.275*

R Core Team (2019). *R: A language and environment for statistical computing*. R Foundation for Statistical Computing, Vienna, Austria. **URL:** *http://www.R-project.org*

Roche CM, Loros JJ, McCluskey K, Glass NL (2014). *Neurospora crassa*: looking back and looking forward at a model microbe. *Am J Bot* **101**: 2022–2035. **URL:** *http://dx.doi.org/10.3732/ajb.1400377*

Roy A, Tamuli R (2022). Heat shock proteins and the calcineurin-crz1 signaling regulate stress responses in fungi. *Archives of Microbiology* **204**: 240.

Sangappillai V, Nadarajah K (2020). Fatty acid synthase beta dehydratase in the lipid biosynthesis pathway is required for conidiogenesis, pigmentation and appressorium formation in *Magnaporthe oryzae* s6. *International Journal of Molecular Sciences* **21**: 7224.

Schulte PM (2015). The effects of temperature on aerobic metabolism: towards a mechanistic understanding of the responses of ectotherms to a changing environment. *Journal of Experimental Biology* **218**: 1856–1866. **URL:** *https://jeb.biologists.org/content/218/12/1856*

Segura V, Vilhjálmsson BJ, Platt A, Korte A, Seren U, Long Q, *et al.* (2012). An efficient multilocus mixed-model approach for genome-wide association studies in structured populations. *Nature Genetics* **44**: 825–830. **URL:** *https://doi.org/10.1038/ng.2314*

Shama LNS, Campero-Paz M, Wegner KM, De Block M, Stoks R (2011). Latitudinal and voltinism compensation shape thermal reaction norms for growth rate. *Molecular Ecology* **20**: 2929–2941. **URL:** *https://onlinelibrary.wiley.com/doi/10.1111/j.1365-294X.2011.05156.x*

Sinclair BJ, Marshall KE, Sewell MA, Levesque DL, Willett CS, Slotsbo S, *et al.* (2016). Can we predict ectotherm responses to climate change using thermal performance curves and body temperatures? *Ecology Letters* **19**: 1372–1385. **URL:** *http://dx.doi.org/10.1111/ele.12686*

Situ J, Zhang X, Zhou X, Zhang Z, Xi P, Kong G, *et al.* (2023). The ankyrin repeat-containing protein PlANK1 mediates mycelial growth, oospore development, and virulence in *Peronophythora litchii*. *Phytopathology Research* **5**: 54.

Slatkin M (2008). Linkage disequilibrium — understanding the evolutionary past and mapping the medical future. *Nat Rev Genet* **9**: 477–485. 1471-0056 10.1038/nrg2361 10.1038/nrg2361. **URL:** *http://dx.doi.org/10.1038/nrg2361*

Suthar M, Dufossé L, Singh SK (2023). The enigmatic world of fungal melanin: a comprehensive review. *Journal of Fungi* **9**: 891.

Sørensen JG, White CR, Duffy GA, Chown SL (2018). A widespread thermodynamic effect, but maintenance of biological rates through space across life's major domains. *Proc Biol Sci* **285**: 20181775.

Taylor J, Butler D (2017). R package asmap: Efficient genetic linkage map construction and diagnosis. *Journal of Statistical Software* **79**: 1–29.

Verdín J, Sánchez-León E, Rico-Ramírez AM, Martínez-Núñez L, Fajardo-Somera RA, Riquelme M (2019). Off the wall: The rhyme and reason of *Neurospora crassa* hyphal morphogenesis. *The Cell Surface* **5**: 100020.

Villalba de la Peña M, Summanen PAM, Liukkonen M, Kronholm I (2023). Chromatin structure influences rate and spectrum of spontaneous mutations in *Neurospora crassa*. *Genome Research* **33**: 1–13. **URL:** *http://genome.cshlp.org/content/early/2023/04/27/gr.276992.122.abstract*

Wang J, Zhang Z (2021). Gapit version 3: Boosting power and accuracy for genomic association and prediction. *Genomics, Proteomics & Bioinformatics* **19**: 629–640. **URL:** *https://www.sciencedirect.com/science/article/pii/S1672022921001777*

Wickham H (2016). *ggplot2: Elegant Graphics for Data Analysis*. Springer-Verlag New York. **URL:** *http://ggplot2.org*

Yamahira K, Kawajiri M, Takeshi K, Irie T (2007). Inter-and intrapopulation variation in thermal reaction norms for growth rate: evolution of latitudinal compensation in ectotherms with a genetic constraint. *Evolution* **61**: 1577–1589.

Yang Y, Xie B, Jing Z, Lu Y, Ye J, Chen Y, *et al.* (2022). *Flammulina filiformis* pkac gene complementing in *Neurospora crassa* mutant reveals its function in mycelial growth and abiotic stress response. *Life* **12**: 1336.

Zhang Z, Ersoz E, Lai CQ, Todhunter RJ, Tiwari HK, Gore MA, *et al.* (2010). Mixed linear model approach adapted for genome-wide association studies. *Nature Genetics* **42**: 355–360. **URL:** *https://doi.org/10.1038/ng.546*

Zhao J, Gladieux P, Hutchison E, Bueche J, Hall C, Perraudeau F, *et al.* (2015). Identification of allorecognition loci in *Neurospora crassa* by genomics and evolutionary approaches. *Molecular Biology and Evolution* **32**: 2417–2432. **URL:** *http://mbe.oxfordjournals.org/content/32/9/2417.abstract*

Supplementary Information

Supplementary Figures

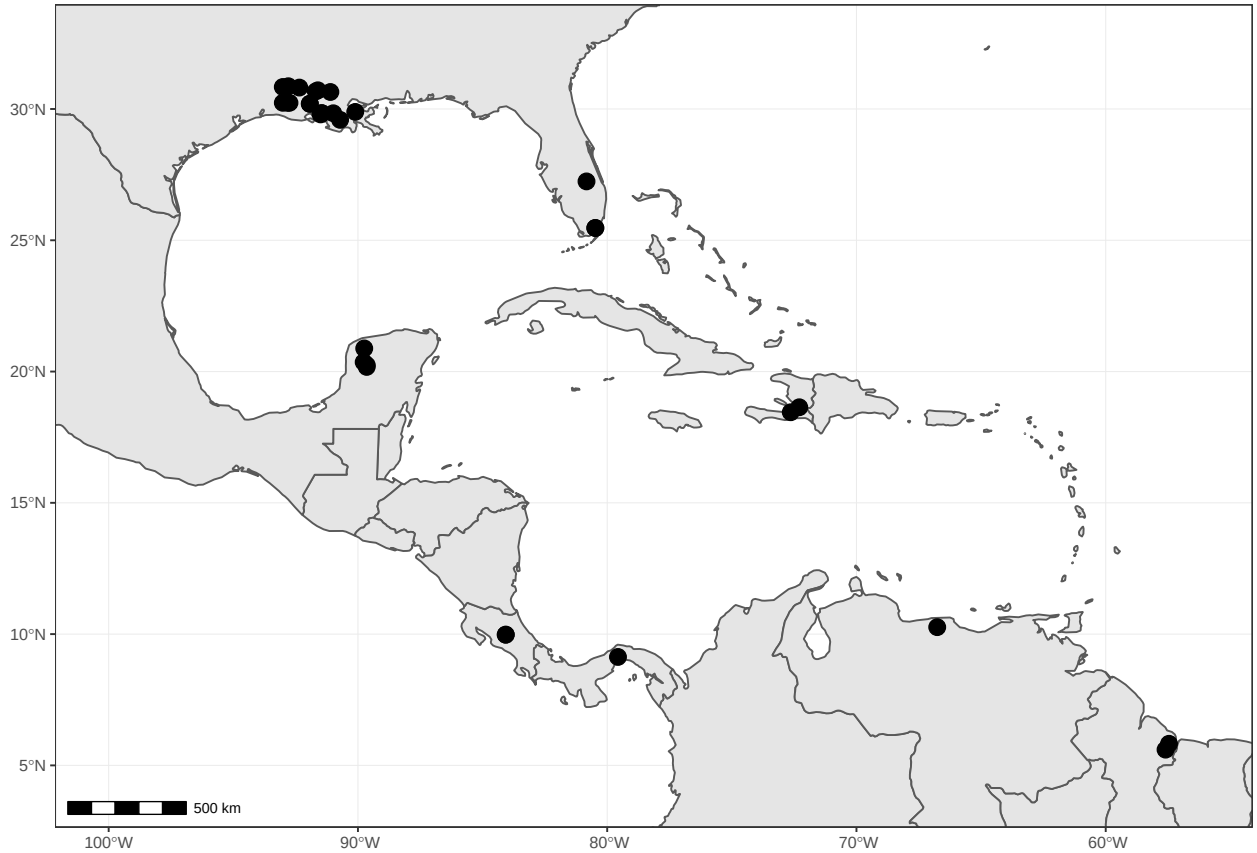

Figure S1: Sampling locations around Southwestern United States and the Caribbean, where the strains originating from nature have been collected.

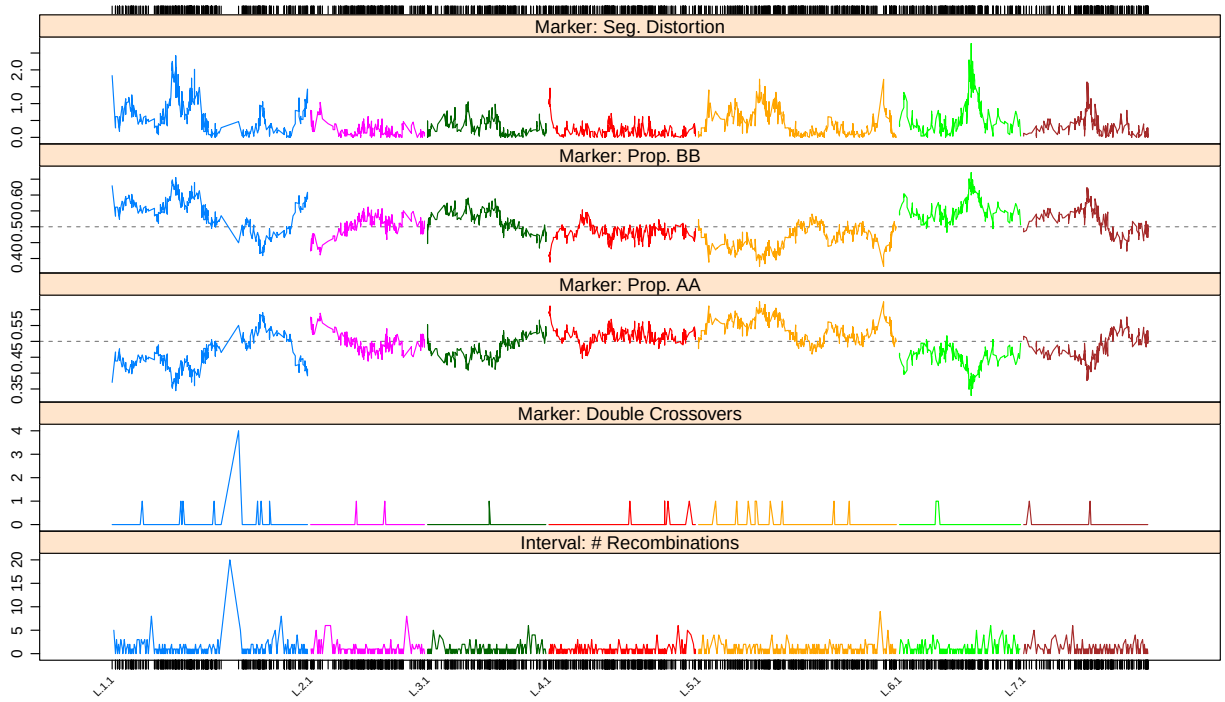

Figure S2: An example of segregation distortion, marker frequencies, doubles crossovers and recombination events in family A offspring. Some double crossover events are observed.

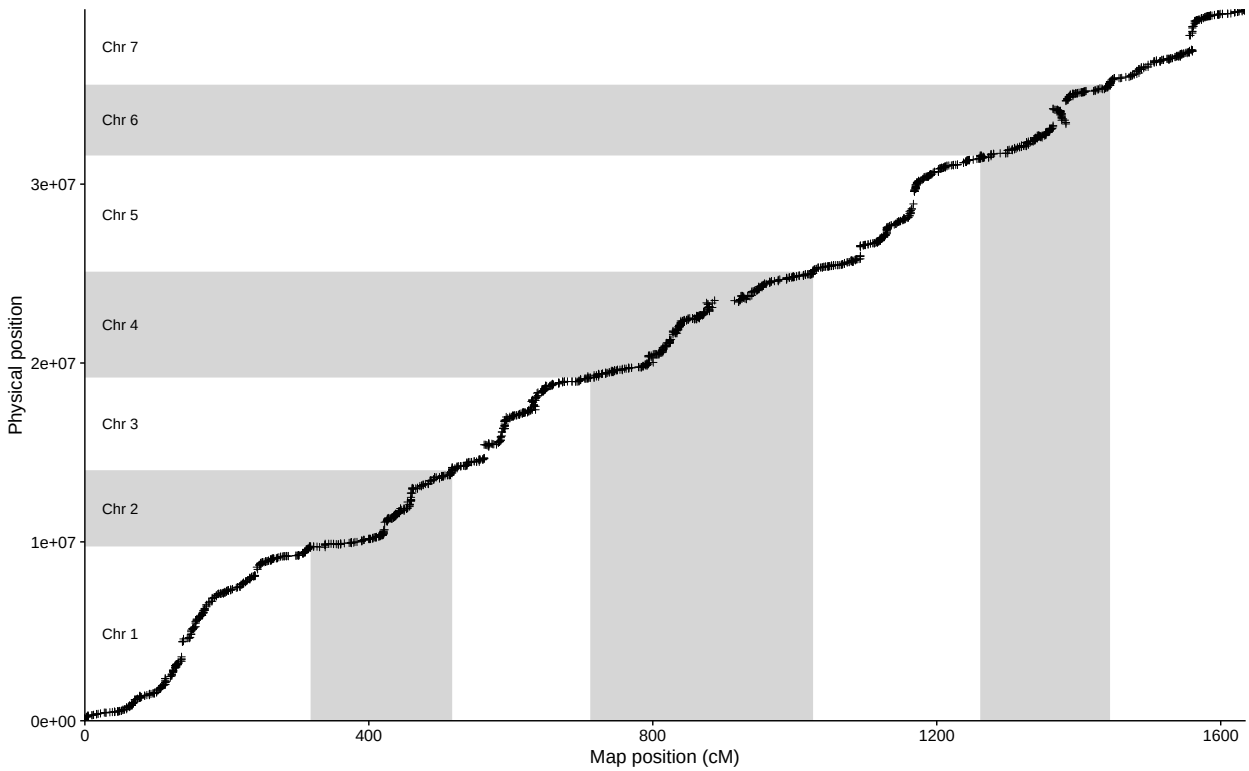

Figure S3: An example of comparing marker order on the genetic map to the physical reference genome for family A. There are only a few cases where markers may be in the wrong order. On chromosome 6 there appears to be an inversion relative to the reference genome.

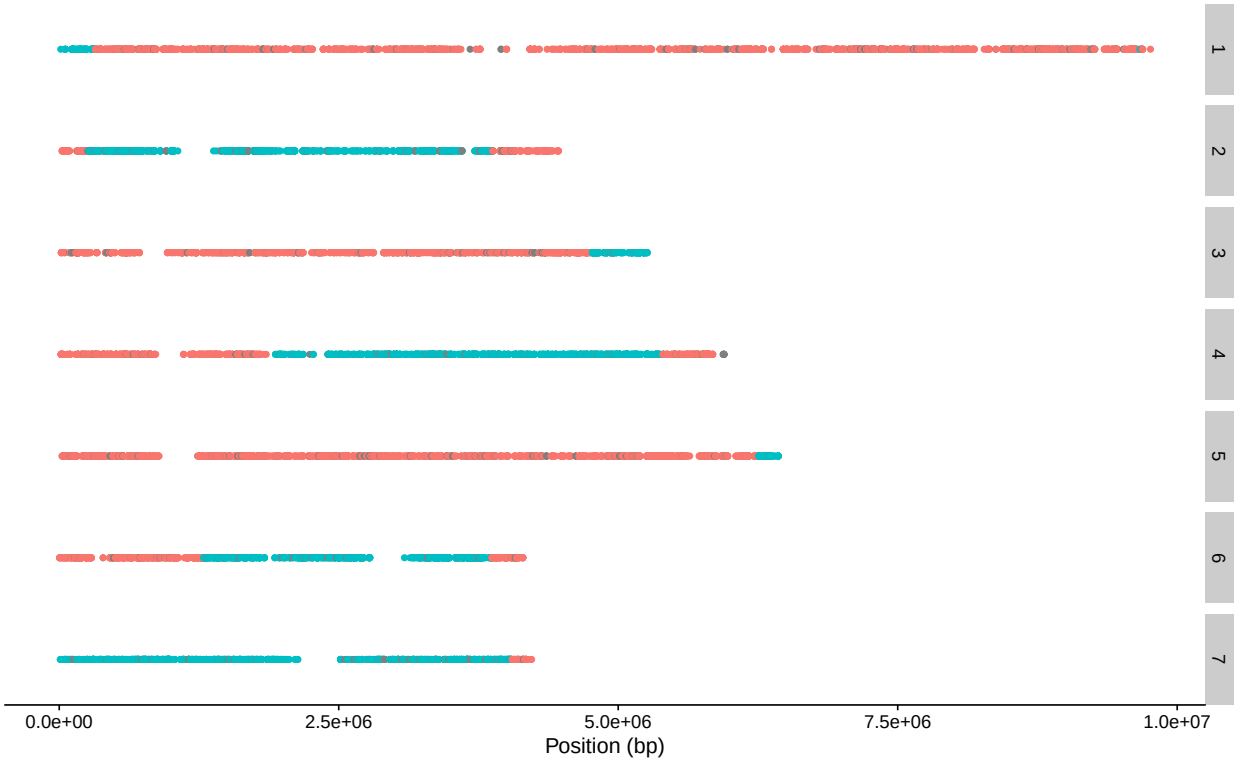

Figure S4: An example of strain A2 with segments of the genome inherited from the two parents: 10886 (red) and 10948 (blue). Grey points are markers with missing data. Facet labeling shows chromosome numbers.

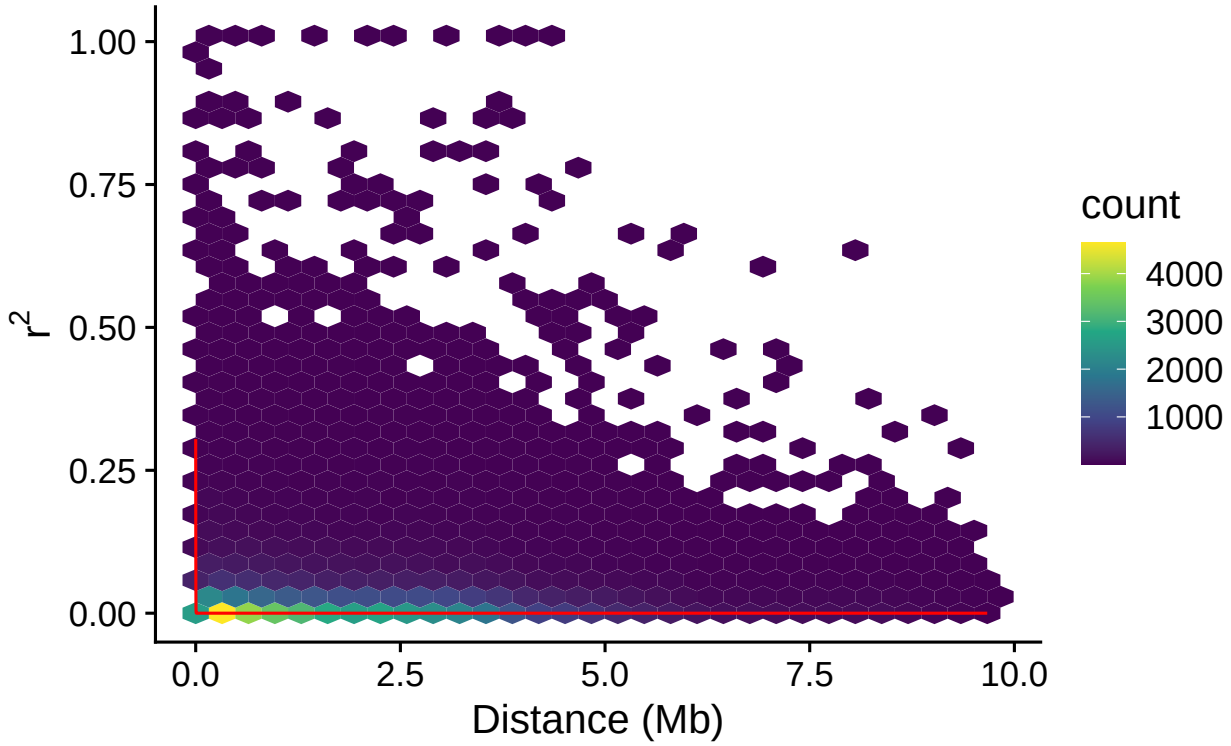

Figure S5: Decay of linkage disequilibrium over long distances across the seven chromosomes of *N. crassa*. We sampled 10 000 pairwise SNP combinations at random from each chromosome, n = 70 000 in total. For plotting data has been binned into hexes. Red line shows exponential decay fit

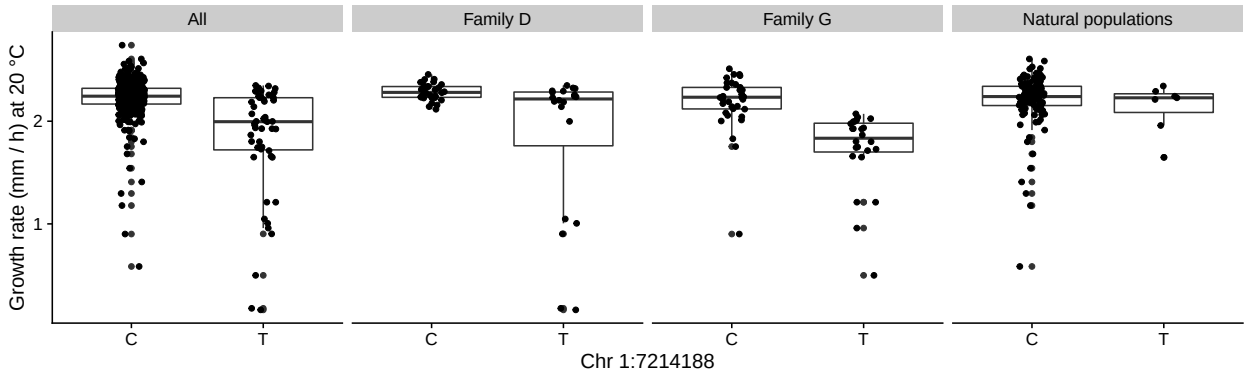

Figure S6: Segregation of SNPs significant at 20 °C.

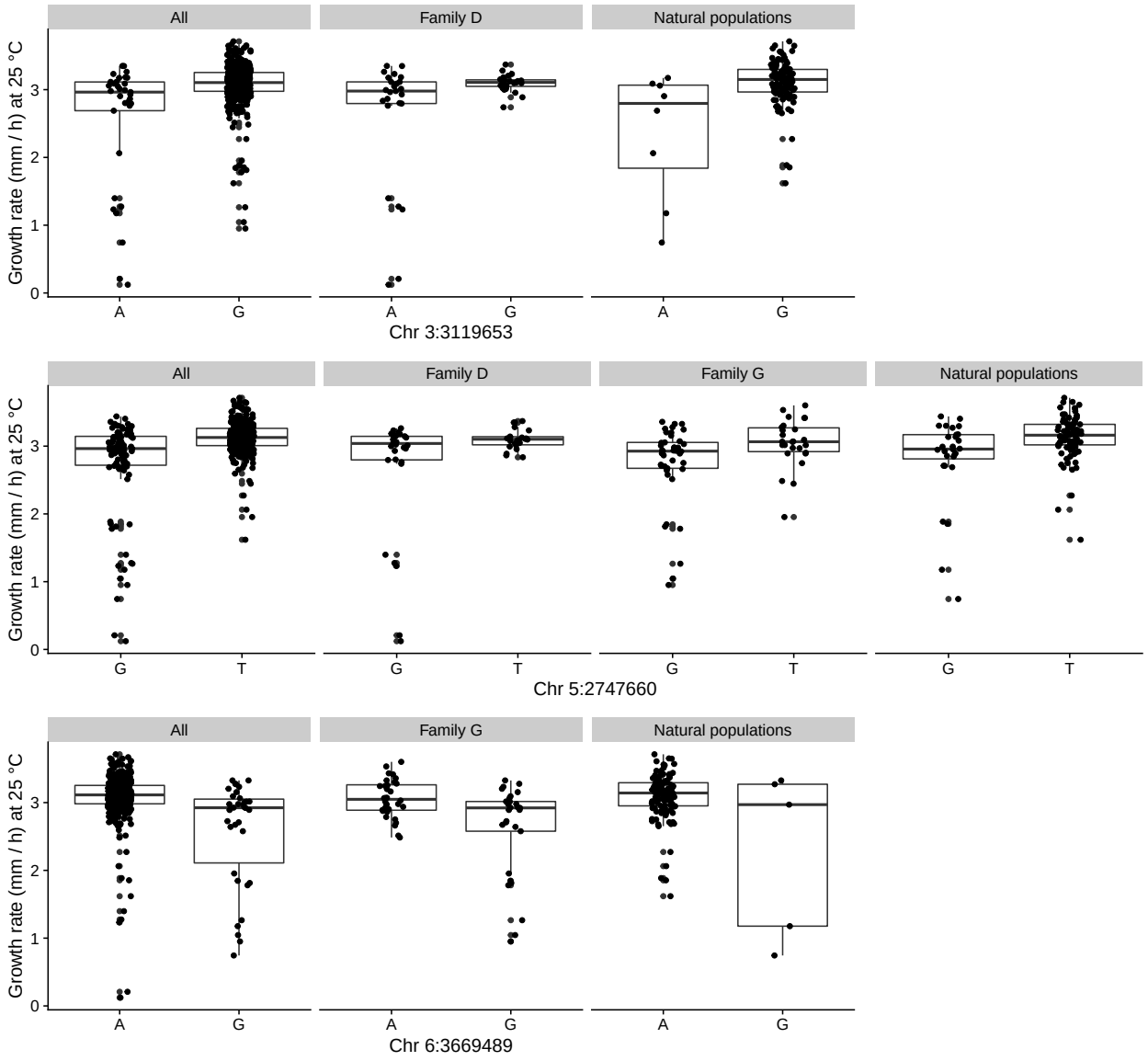

Figure S7: Segregation of SNPs significant at 25 °C.

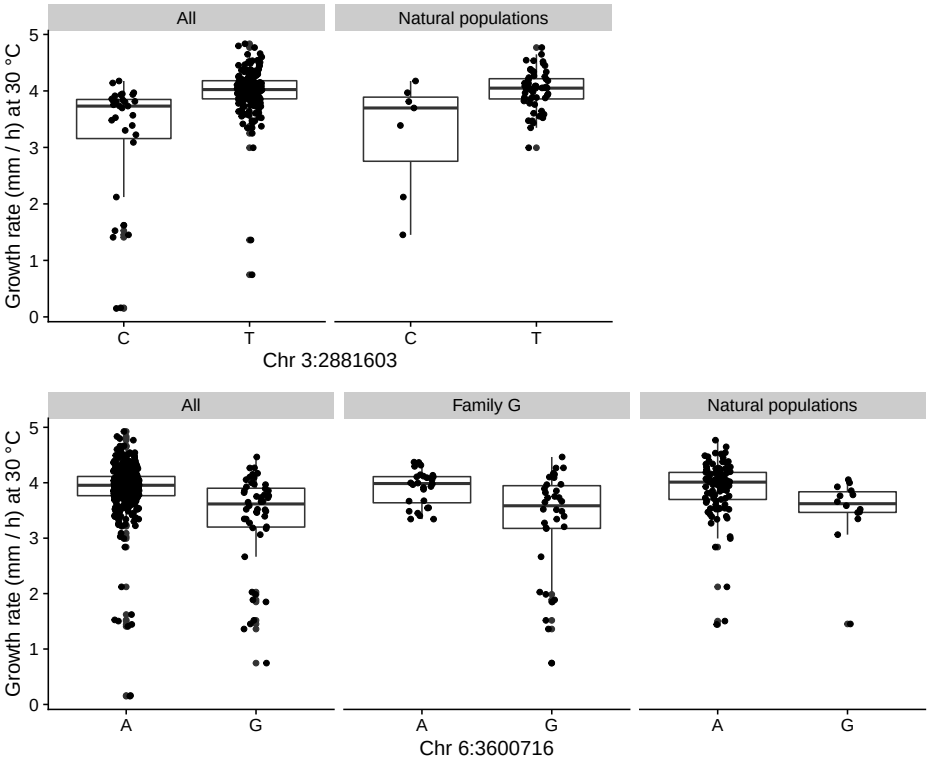

Figure S8: Segregation of SNPs significant at 30 °C.

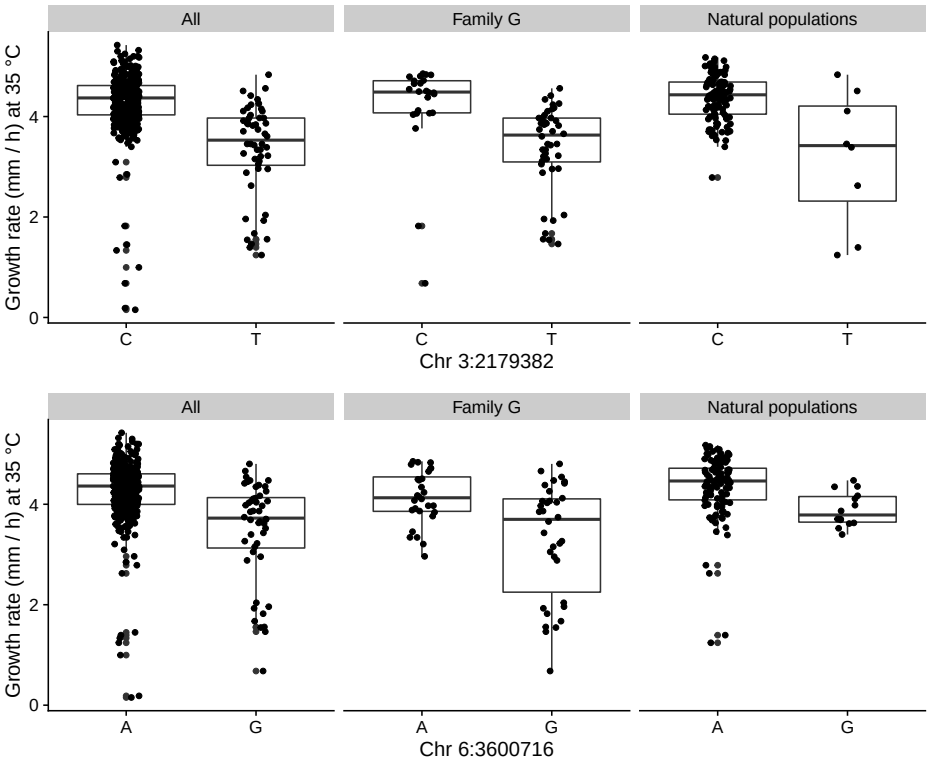

Figure S9: Segregation of SNPs significant at 35 °C.

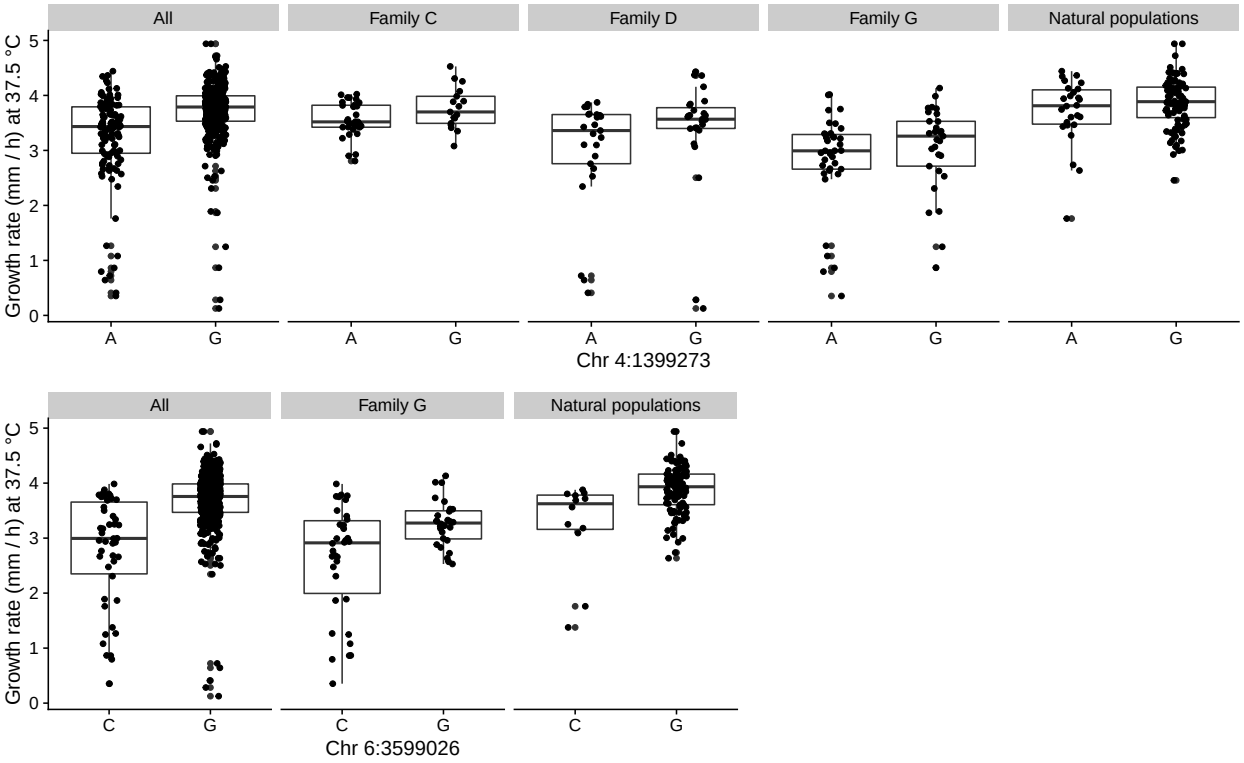

Figure S10: Segregation of SNPs significant at 37.5 °C.

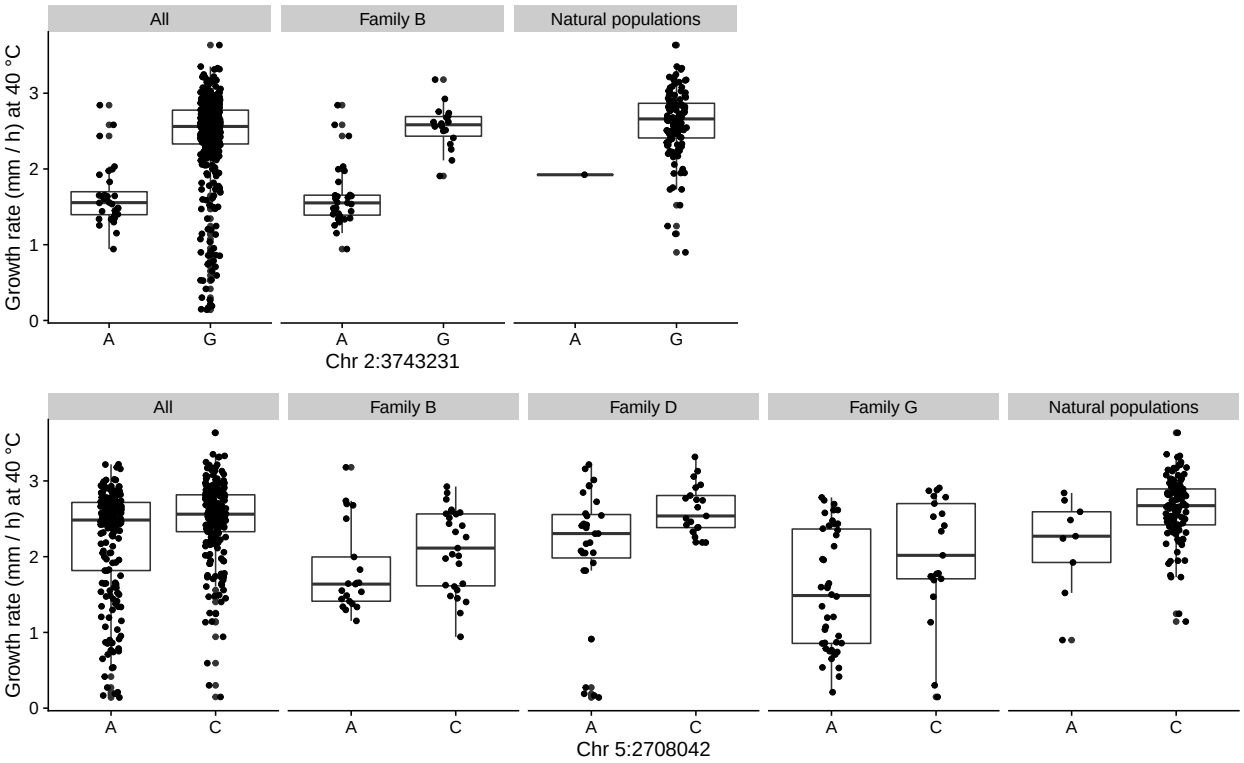

Figure S11: Segregation of SNPs significant at 40 °C.

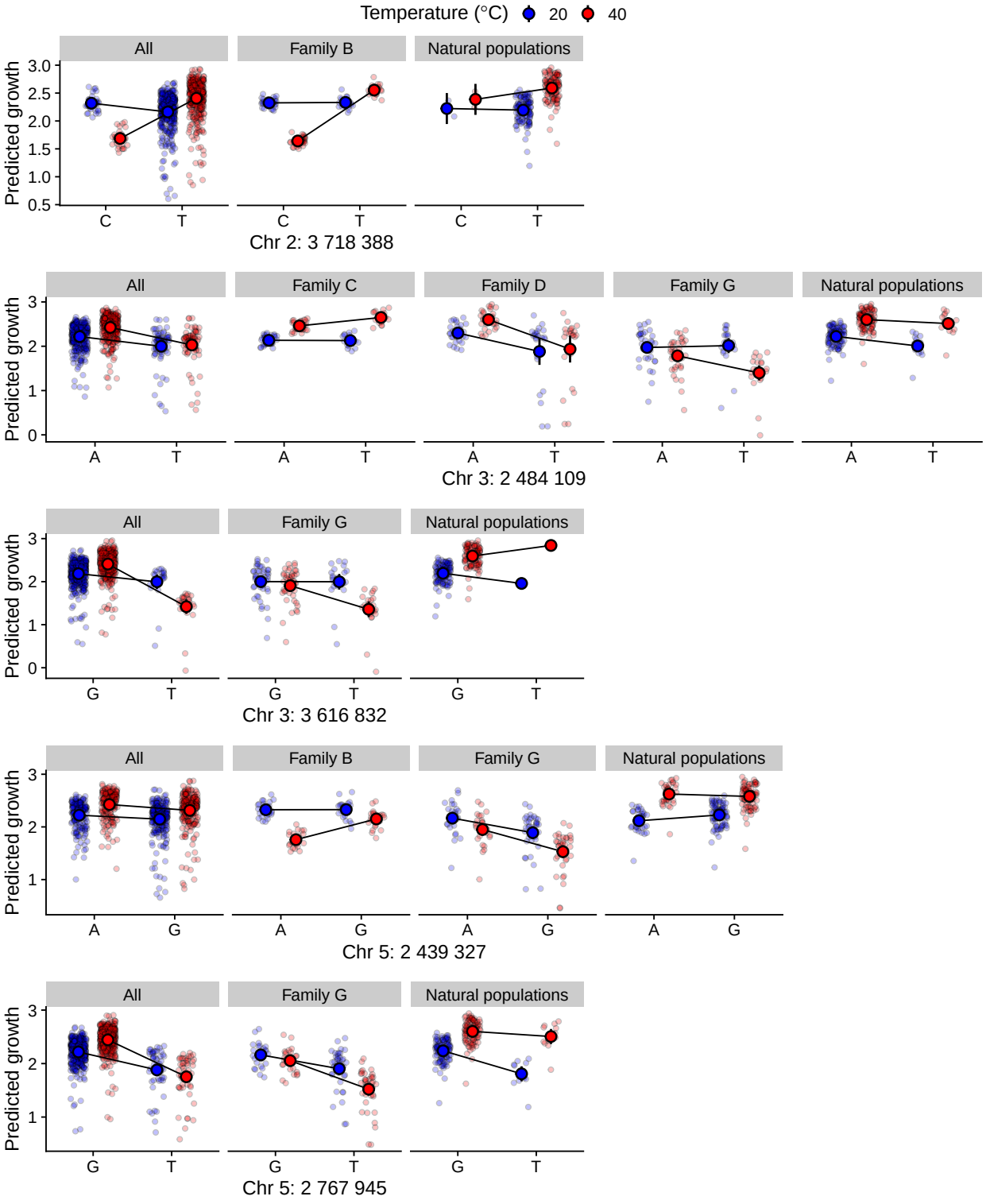

Figure S12: Allelic effects for SNPs associated with TPC breadth, that have no evidence of trade-offs between 20 and 40 °C.

Supplementary Tables

Table S1: List of strains. Column origin indicates whether the strain was sampled from a natural population or if it was from a family obtained by crossing two natural strains. Column source indicates which strains were obtained from the Fungal Genetics Stock Center (FGSC) and which were generated in Moghadam *et al.* 2020. LA = Louisiana, USA. FL = Florida, USA. Strains 10948 and 10886 are parents of family A, 10932 and 1165 are parents of family B, 4498 and 8816 are parents of family C, 3223 and 8845 are parents of family D, and 10904 and 851 are parents of family G.

Strain	Origin	Source	Collection site
847	Natural population	FGSC	LA
851	Natural population	FGSC	Costa Rica
1131	Natural population	FGSC	Panama
1132	Natural population	FGSC	Panama
1133	Natural population	FGSC	Panama
1165	Natural population	FGSC	Panama
2229	Natural population	FGSC	Welsh, LA
2489	Laboratory strain	FGSC	Marrero, LA
3200	Natural population	FGSC	Coon, LA
3210	Natural population	FGSC	Sugartown, LA
3211	Natural population	FGSC	Sugartown, LA
3212	Natural population	FGSC	Ravenswood, LA
3223	Natural population	FGSC	Elizabeth, LA
3943	Natural population	FGSC	Houma, LA
3968	Natural population	FGSC	Okeechobee, FL
3975	Natural population	FGSC	FL
4494	Natural population	FGSC	Franklin, LA
4498	Natural population	FGSC	Franklin, LA
4708	Natural population	FGSC	Haiti
4712	Natural population	FGSC	Haiti
4713	Natural population	FGSC	Haiti
4715	Natural population	FGSC	Haiti
4716	Natural population	FGSC	Haiti
4730	Natural population	FGSC	Venezuela
4824	Natural population	FGSC	Haiti
5910	Natural population	FGSC	Digitima Creek, Guyana
5914	Natural population	FGSC	Torani Canal, Guyana
6203	Natural population	FGSC	Aguda Rd, Costa Rica
7833	Natural population	FGSC	Houma, LA
8783	Natural population	FGSC	Homestead, FL
8784	Natural population	FGSC	Homestead, FL
8787	Natural population	FGSC	Homestead, FL

Continued on next page…

Table S1 – Continued

Strain	Origin	Source	Collection site
8789	Natural population	FGSC	Homestead, FL
8790	Natural population	FGSC	Homestead, FL
8816	Natural population	FGSC	Carrefour Dufort, Haiti
8819	Natural population	FGSC	Carrefour Dufort, Haiti
8829	Natural population	FGSC	Tiassale, Ivory Coast
8845	Natural population	FGSC	Kabah, Yucatan, Mexico
8848	Natural population	FGSC	Sayil, Yucatan, Mexico
8850	Natural population	FGSC	Uxmal, Yucatan, Mexico
8851	Natural population	FGSC	Uman, Yucatan, Mexico
10881	Natural population	FGSC	Franklin, LA
10882	Natural population	FGSC	Franklin, LA
10883	Natural population	FGSC	Franklin, LA
10884	Natural population	FGSC	Franklin, LA
10885	Natural population	FGSC	Franklin, LA
10886	Natural population	FGSC	Franklin, LA
10887	Natural population	FGSC	Franklin, LA
10888	Natural population	FGSC	Franklin, LA
10889	Natural population	FGSC	Franklin, LA
10890	Natural population	FGSC	Marrero, LA
10891	Natural population	FGSC	Welsh, LA
10892	Natural population	FGSC	Northside Planting, LA
10893	Natural population	FGSC	Houma, LA
10894	Natural population	FGSC	Houma, LA
10895	Natural population	FGSC	Welsh, LA
10896	Natural population	FGSC	Iowa, LA
10897	Natural population	FGSC	Iowa, LA
10898	Natural population	FGSC	Iowa, LA
10899	Natural population	FGSC	Marrero, LA
10900	Natural population	FGSC	Houma, LA
10901	Natural population	FGSC	Houma, LA
10902	Natural population	FGSC	Houma, LA
10903	Natural population	FGSC	Houma, LA
10904	Natural population	FGSC	Houma, LA
10905	Natural population	FGSC	Welsh, LA
10906	Natural population	FGSC	Roanoke, LA
10907	Natural population	FGSC	Roanoke, LA
10908	Natural population	FGSC	Roanoke, LA
10909	Natural population	FGSC	Iowa, LA
10910	Natural population	FGSC	Iowa, LA
10911	Natural population	FGSC	Elizabeth, LA
10912	Natural population	FGSC	Elizabeth, LA
10914	Natural population	FGSC	Northside Plantation, LA
10915	Natural population	FGSC	Franklin, LA
10916	Natural population	FGSC	Houma, LA
10917	Natural population	FGSC	Elizabeth, LA

Continued on next page…

Table S1 – Continued

Strain	Origin	Source	Collection site
10918	Natural population	FGSC	Bayou Chicot, LA
10919	Natural population	FGSC	Coon, LA
10920	Natural population	FGSC	Fred, LA
10921	Natural population	FGSC	Franklin, LA
10922	Natural population	FGSC	Welsh, LA
10923	Natural population	FGSC	Welsh, LA
10925	Natural population	FGSC	Roanoke, LA
10926	Natural population	FGSC	Coon, LA
10927	Natural population	FGSC	Coon, LA
10928	Natural population	FGSC	Georgia Plantation, LA
10929	Natural population	FGSC	Georgia Plantation, LA
10930	Natural population	FGSC	Houma, LA
10931	Natural population	FGSC	Houma, LA
10932	Natural population	FGSC	Welsh, LA
10934	Natural population	FGSC	Roanoke, LA
10935	Natural population	FGSC	Welsh, LA
10936	Natural population	FGSC	Welsh, LA
10937	Natural population	FGSC	Welsh, LA
10938	Natural population	FGSC	Roanoke, LA
10939	Natural population	FGSC	Sugartown, LA
10941	Natural population	FGSC	Iowa, LA
10942	Natural population	FGSC	Iowa, LA
10943	Natural population	FGSC	Iowa, LA
10946	Natural population	FGSC	Elizabeth, LA
10948	Natural population	FGSC	Bayou Chicot, LA
10950	Natural population	FGSC	Coon, LA
10951	Natural population	FGSC	Coon, LA
10954	Natural population	FGSC	Roanoke, LA
10982	Natural population	FGSC	Roanoke, LA
10983	Natural population	FGSC	Elizabeth, LA
26805	Natural population	FGSC	Iowa, LA
26806	Natural population	FGSC	Marrero, LA
26807	Natural population	FGSC	Houma, LA
26808	Natural population	FGSC	Houma, LA
26809	Natural population	FGSC	Houma, LA
26810	Natural population	FGSC	Welsh, LA
26811	Natural population	FGSC	Roanoke, LA
26812	Natural population	FGSC	Iowa, LA
26813	Natural population	FGSC	Elizabeth, LA
26814	Natural population	FGSC	Elizabeth, LA
26815	Natural population	FGSC	Houma, LA
A1	Family A	Moghadam *et al.* 2020	-
A2	Family A	Moghadam *et al.* 2020	-
A3	Family A	Moghadam *et al.* 2020	-
A4	Family A	Moghadam *et al.* 2020	-

Continued on next page…

Table S1 – Continued

Strain	Origin	Source	Collection site
A5	Family A	Moghadam *et al.* 2020	-
A6	Family A	Moghadam *et al.* 2020	-
A7	Family A	Moghadam *et al.* 2020	-
A8	Family A	Moghadam *et al.* 2020	-
A9	Family A	Moghadam *et al.* 2020	-
A10	Family A	Moghadam *et al.* 2020	-
A11	Family A	Moghadam *et al.* 2020	-
A12	Family A	Moghadam *et al.* 2020	-
A13	Family A	Moghadam *et al.* 2020	-
A14	Family A	Moghadam *et al.* 2020	-
A15	Family A	Moghadam *et al.* 2020	-
A16	Family A	Moghadam *et al.* 2020	-
A17	Family A	Moghadam *et al.* 2020	-
A18	Family A	Moghadam *et al.* 2020	-
A19	Family A	Moghadam *et al.* 2020	-
A20	Family A	Moghadam *et al.* 2020	-
A21	Family A	Moghadam *et al.* 2020	-
A22	Family A	Moghadam *et al.* 2020	-
A23	Family A	Moghadam *et al.* 2020	-
A24	Family A	Moghadam *et al.* 2020	-
A25	Family A	Moghadam *et al.* 2020	-
A26	Family A	Moghadam *et al.* 2020	-
A27	Family A	Moghadam *et al.* 2020	-
A28	Family A	Moghadam *et al.* 2020	-
A29	Family A	Moghadam *et al.* 2020	-
A30	Family A	Moghadam *et al.* 2020	-
A31	Family A	Moghadam *et al.* 2020	-
A32	Family A	Moghadam *et al.* 2020	-
A33	Family A	Moghadam *et al.* 2020	-
A34	Family A	Moghadam *et al.* 2020	-
A35	Family A	Moghadam *et al.* 2020	-
A36	Family A	Moghadam *et al.* 2020	-
A37	Family A	Moghadam *et al.* 2020	-
A38	Family A	Moghadam *et al.* 2020	-
A39	Family A	Moghadam *et al.* 2020	-
A40	Family A	Moghadam *et al.* 2020	-
A41	Family A	Moghadam *et al.* 2020	-
A42	Family A	Moghadam *et al.* 2020	-
A43	Family A	Moghadam *et al.* 2020	-
A44	Family A	Moghadam *et al.* 2020	-
A45	Family A	Moghadam *et al.* 2020	-
A46	Family A	Moghadam *et al.* 2020	-
A47	Family A	Moghadam *et al.* 2020	-
A48	Family A	Moghadam *et al.* 2020	-
A49	Family A	Moghadam *et al.* 2020	-

Continued on next page…

Table S1 – Continued

Strain	Origin	Source	Collection site
A50	Family A	Moghadam *et al.* 2020	-
A51	Family A	Moghadam *et al.* 2020	-
A52	Family A	Moghadam *et al.* 2020	-
A53	Family A	Moghadam *et al.* 2020	-
A54	Family A	Moghadam *et al.* 2020	-
A55	Family A	Moghadam *et al.* 2020	-
A56	Family A	Moghadam *et al.* 2020	-
A57	Family A	Moghadam *et al.* 2020	-
A58	Family A	Moghadam *et al.* 2020	-
A59	Family A	Moghadam *et al.* 2020	-
A60	Family A	Moghadam *et al.* 2020	-
A61	Family A	Moghadam *et al.* 2020	-
A62	Family A	Moghadam *et al.* 2020	-
A63	Family A	Moghadam *et al.* 2020	-
A64	Family A	Moghadam *et al.* 2020	-
A65	Family A	Moghadam *et al.* 2020	-
A66	Family A	Moghadam *et al.* 2020	-
A67	Family A	Moghadam *et al.* 2020	-
A68	Family A	Moghadam *et al.* 2020	-
A69	Family A	Moghadam *et al.* 2020	-
A70	Family A	Moghadam *et al.* 2020	-
A71	Family A	Moghadam *et al.* 2020	-
A72	Family A	Moghadam *et al.* 2020	-
A73	Family A	Moghadam *et al.* 2020	-
A74	Family A	Moghadam *et al.* 2020	-
A75	Family A	Moghadam *et al.* 2020	-
A76	Family A	Moghadam *et al.* 2020	-
A77	Family A	Moghadam *et al.* 2020	-
A78	Family A	Moghadam *et al.* 2020	-
A79	Family A	Moghadam *et al.* 2020	-
A80	Family A	Moghadam *et al.* 2020	-
A81	Family A	Moghadam *et al.* 2020	-
A82	Family A	Moghadam *et al.* 2020	-
A83	Family A	Moghadam *et al.* 2020	-
A84	Family A	Moghadam *et al.* 2020	-
A85	Family A	Moghadam *et al.* 2020	-
A86	Family A	Moghadam *et al.* 2020	-
A87	Family A	Moghadam *et al.* 2020	-
A88	Family A	Moghadam *et al.* 2020	-
A89	Family A	Moghadam *et al.* 2020	-
A90	Family A	Moghadam *et al.* 2020	-
A91	Family A	Moghadam *et al.* 2020	-
A92	Family A	Moghadam *et al.* 2020	-
A93	Family A	Moghadam *et al.* 2020	-
A94	Family A	Moghadam *et al.* 2020	-

Continued on next page…

Table S1 – Continued

Strain	Origin	Source	Collection site
B1	Family B	Moghadam *et al.* 2020	-
B2	Family B	Moghadam *et al.* 2020	-
B3	Family B	Moghadam *et al.* 2020	-
B4	Family B	Moghadam *et al.* 2020	-
B5	Family B	Moghadam *et al.* 2020	-
B6	Family B	Moghadam *et al.* 2020	-
B7	Family B	Moghadam *et al.* 2020	-
B8	Family B	Moghadam *et al.* 2020	-
B9	Family B	Moghadam *et al.* 2020	-
B10	Family B	Moghadam *et al.* 2020	-
B11	Family B	Moghadam *et al.* 2020	-
B12	Family B	Moghadam *et al.* 2020	-
B13	Family B	Moghadam *et al.* 2020	-
B14	Family B	Moghadam *et al.* 2020	-
B15	Family B	Moghadam *et al.* 2020	-
B16	Family B	Moghadam *et al.* 2020	-
B17	Family B	Moghadam *et al.* 2020	-
B18	Family B	Moghadam *et al.* 2020	-
B19	Family B	Moghadam *et al.* 2020	-
B20	Family B	Moghadam *et al.* 2020	-
B21	Family B	Moghadam *et al.* 2020	-
B22	Family B	Moghadam *et al.* 2020	-
B23	Family B	Moghadam *et al.* 2020	-
B24	Family B	Moghadam *et al.* 2020	-
B25	Family B	Moghadam *et al.* 2020	-
B26	Family B	Moghadam *et al.* 2020	-
B27	Family B	Moghadam *et al.* 2020	-
B28	Family B	Moghadam *et al.* 2020	-
B29	Family B	Moghadam *et al.* 2020	-
B30	Family B	Moghadam *et al.* 2020	-
B31	Family B	Moghadam *et al.* 2020	-
B32	Family B	Moghadam *et al.* 2020	-
B33	Family B	Moghadam *et al.* 2020	-
B34	Family B	Moghadam *et al.* 2020	-
B35	Family B	Moghadam *et al.* 2020	-
B36	Family B	Moghadam *et al.* 2020	-
B37	Family B	Moghadam *et al.* 2020	-
B38	Family B	Moghadam *et al.* 2020	-
B39	Family B	Moghadam *et al.* 2020	-
B40	Family B	Moghadam *et al.* 2020	-
B41	Family B	Moghadam *et al.* 2020	-
B42	Family B	Moghadam *et al.* 2020	-
B43	Family B	Moghadam *et al.* 2020	-
B44	Family B	Moghadam *et al.* 2020	-
B45	Family B	Moghadam *et al.* 2020	-

Continued on next page…

Table S1 – Continued

Strain	Origin	Source	Collection site
B46	Family B	Moghadam *et al.* 2020	-
B47	Family B	Moghadam *et al.* 2020	-
B48	Family B	Moghadam *et al.* 2020	-
B49	Family B	Moghadam *et al.* 2020	-
B50	Family B	Moghadam *et al.* 2020	-
C1	Family C	Moghadam *et al.* 2020	-
C2	Family C	Moghadam *et al.* 2020	-
C3	Family C	Moghadam *et al.* 2020	-
C4	Family C	Moghadam *et al.* 2020	-
C5	Family C	Moghadam *et al.* 2020	-
C6	Family C	Moghadam *et al.* 2020	-
C7	Family C	Moghadam *et al.* 2020	-
C8	Family C	Moghadam *et al.* 2020	-
C9	Family C	Moghadam *et al.* 2020	-
C10	Family C	Moghadam *et al.* 2020	-
C11	Family C	Moghadam *et al.* 2020	-
C12	Family C	Moghadam *et al.* 2020	-
C13	Family C	Moghadam *et al.* 2020	-
C14	Family C	Moghadam *et al.* 2020	-
C15	Family C	Moghadam *et al.* 2020	-
C16	Family C	Moghadam *et al.* 2020	-
C17	Family C	Moghadam *et al.* 2020	-
C18	Family C	Moghadam *et al.* 2020	-
C19	Family C	Moghadam *et al.* 2020	-
C20	Family C	Moghadam *et al.* 2020	-
C21	Family C	Moghadam *et al.* 2020	-
C22	Family C	Moghadam *et al.* 2020	-
C23	Family C	Moghadam *et al.* 2020	-
C24	Family C	Moghadam *et al.* 2020	-
C25	Family C	Moghadam *et al.* 2020	-
C26	Family C	Moghadam *et al.* 2020	-
C27	Family C	Moghadam *et al.* 2020	-
C28	Family C	Moghadam *et al.* 2020	-
C29	Family C	Moghadam *et al.* 2020	-
C30	Family C	Moghadam *et al.* 2020	-
C31	Family C	Moghadam *et al.* 2020	-
C32	Family C	Moghadam *et al.* 2020	-
C33	Family C	Moghadam *et al.* 2020	-
C34	Family C	Moghadam *et al.* 2020	-
C35	Family C	Moghadam *et al.* 2020	-
C36	Family C	Moghadam *et al.* 2020	-
C37	Family C	Moghadam *et al.* 2020	-
C38	Family C	Moghadam *et al.* 2020	-
C39	Family C	Moghadam *et al.* 2020	-
C40	Family C	Moghadam *et al.* 2020	-

Continued on next page…

Table S1 – Continued

Strain	Origin	Source	Collection site
C41	Family C	Moghadam *et al.* 2020	-
C42	Family C	Moghadam *et al.* 2020	-
C43	Family C	Moghadam *et al.* 2020	-
C44	Family C	Moghadam *et al.* 2020	-
C45	Family C	Moghadam *et al.* 2020	-
C46	Family C	Moghadam *et al.* 2020	-
C47	Family C	Moghadam *et al.* 2020	-
C48	Family C	Moghadam *et al.* 2020	-
C49	Family C	Moghadam *et al.* 2020	-
C50	Family C	Moghadam *et al.* 2020	-
D1	Family D	Moghadam *et al.* 2020	-
D2	Family D	Moghadam *et al.* 2020	-
D3	Family D	Moghadam *et al.* 2020	-
D4	Family D	Moghadam *et al.* 2020	-
D5	Family D	Moghadam *et al.* 2020	-
D6	Family D	Moghadam *et al.* 2020	-
D7	Family D	Moghadam *et al.* 2020	-
D8	Family D	Moghadam *et al.* 2020	-
D9	Family D	Moghadam *et al.* 2020	-
D10	Family D	Moghadam *et al.* 2020	-
D11	Family D	Moghadam *et al.* 2020	-
D12	Family D	Moghadam *et al.* 2020	-
D13	Family D	Moghadam *et al.* 2020	-
D14	Family D	Moghadam *et al.* 2020	-
D15	Family D	Moghadam *et al.* 2020	-
D16	Family D	Moghadam *et al.* 2020	-
D17	Family D	Moghadam *et al.* 2020	-
D18	Family D	Moghadam *et al.* 2020	-
D19	Family D	Moghadam *et al.* 2020	-
D20	Family D	Moghadam *et al.* 2020	-
D21	Family D	Moghadam *et al.* 2020	-
D22	Family D	Moghadam *et al.* 2020	-
D23	Family D	Moghadam *et al.* 2020	-
D24	Family D	Moghadam *et al.* 2020	-
D25	Family D	Moghadam *et al.* 2020	-
D26	Family D	Moghadam *et al.* 2020	-
D27	Family D	Moghadam *et al.* 2020	-
D28	Family D	Moghadam *et al.* 2020	-
D29	Family D	Moghadam *et al.* 2020	-
D30	Family D	Moghadam *et al.* 2020	-
D31	Family D	Moghadam *et al.* 2020	-
D32	Family D	Moghadam *et al.* 2020	-
D33	Family D	Moghadam *et al.* 2020	-
D34	Family D	Moghadam *et al.* 2020	-
D35	Family D	Moghadam *et al.* 2020	-

Continued on next page…

Table S1 – Continued

Strain	Origin	Source	Collection site
D36	Family D	Moghadam *et al.* 2020	-
D37	Family D	Moghadam *et al.* 2020	-
D38	Family D	Moghadam *et al.* 2020	-
D39	Family D	Moghadam *et al.* 2020	-
D40	Family D	Moghadam *et al.* 2020	-
D41	Family D	Moghadam *et al.* 2020	-
D42	Family D	Moghadam *et al.* 2020	-
D43	Family D	Moghadam *et al.* 2020	-
D44	Family D	Moghadam *et al.* 2020	-
D45	Family D	Moghadam *et al.* 2020	-
D46	Family D	Moghadam *et al.* 2020	-
D47	Family D	Moghadam *et al.* 2020	-
D48	Family D	Moghadam *et al.* 2020	-
D49	Family D	Moghadam *et al.* 2020	-
D50	Family D	Moghadam *et al.* 2020	-
D51	Family D	Moghadam *et al.* 2020	-
D52	Family D	Moghadam *et al.* 2020	-
G1	Family G	Moghadam *et al.* 2020	-
G3	Family G	Moghadam *et al.* 2020	-
G4	Family G	Moghadam *et al.* 2020	-
G5	Family G	Moghadam *et al.* 2020	-
G6	Family G	Moghadam *et al.* 2020	-
G7	Family G	Moghadam *et al.* 2020	-
G8	Family G	Moghadam *et al.* 2020	-
G9	Family G	Moghadam *et al.* 2020	-
G10	Family G	Moghadam *et al.* 2020	-
G11	Family G	Moghadam *et al.* 2020	-
G12	Family G	Moghadam *et al.* 2020	-
G13	Family G	Moghadam *et al.* 2020	-
G14	Family G	Moghadam *et al.* 2020	-
G15	Family G	Moghadam *et al.* 2020	-
G16	Family G	Moghadam *et al.* 2020	-
G17	Family G	Moghadam *et al.* 2020	-
G18	Family G	Moghadam *et al.* 2020	-
G19	Family G	Moghadam *et al.* 2020	-
G20	Family G	Moghadam *et al.* 2020	-
G21	Family G	Moghadam *et al.* 2020	-
G22	Family G	Moghadam *et al.* 2020	-
G23	Family G	Moghadam *et al.* 2020	-
G24	Family G	Moghadam *et al.* 2020	-
G25	Family G	Moghadam *et al.* 2020	-
G26	Family G	Moghadam *et al.* 2020	-
G27	Family G	Moghadam *et al.* 2020	-
G28	Family G	Moghadam *et al.* 2020	-
G29	Family G	Moghadam *et al.* 2020	-

Continued on next page…

Table S1 – Continued

Strain	Origin	Source	Collection site
G30	Family G	Moghadam *et al.* 2020	-
G31	Family G	Moghadam *et al.* 2020	-
G32	Family G	Moghadam *et al.* 2020	-
G33	Family G	Moghadam *et al.* 2020	-
G34	Family G	Moghadam *et al.* 2020	-
G35	Family G	Moghadam *et al.* 2020	-
G36	Family G	Moghadam *et al.* 2020	-
G37	Family G	Moghadam *et al.* 2020	-
G38	Family G	Moghadam *et al.* 2020	-
G39	Family G	Moghadam *et al.* 2020	-
G40	Family G	Moghadam *et al.* 2020	-
G41	Family G	Moghadam *et al.* 2020	-
G42	Family G	Moghadam *et al.* 2020	-
G43	Family G	Moghadam *et al.* 2020	-
G44	Family G	Moghadam *et al.* 2020	-
G45	Family G	Moghadam *et al.* 2020	-
G46	Family G	Moghadam *et al.* 2020	-
G47	Family G	Moghadam *et al.* 2020	-
G48	Family G	Moghadam *et al.* 2020	-
G49	Family G	Moghadam *et al.* 2020	-
G50	Family G	Moghadam *et al.* 2020	-
G52	Family G	Moghadam *et al.* 2020	-
G53	Family G	Moghadam *et al.* 2020	-
G54	Family G	Moghadam *et al.* 2020	-
G55	Family G	Moghadam *et al.* 2020	-
G56	Family G	Moghadam *et al.* 2020	-
G57	Family G	Moghadam *et al.* 2020	-
G58	Family G	Moghadam *et al.* 2020	-
G59	Family G	Moghadam *et al.* 2020	-
G60	Family G	Moghadam *et al.* 2020	-
G61	Family G	Moghadam *et al.* 2020	-
G62	Family G	Moghadam *et al.* 2020	-
G63	Family G	Moghadam *et al.* 2020	-
G64	Family G	Moghadam *et al.* 2020	-
G65	Family G	Moghadam *et al.* 2020	-
G66	Family G	Moghadam *et al.* 2020	-
G67	Family G	Moghadam *et al.* 2020	-
G68	Family G	Moghadam *et al.* 2020	-
G69	Family G	Moghadam *et al.* 2020	-
G70	Family G	Moghadam *et al.* 2020	-
G71	Family G	Moghadam *et al.* 2020	-
G72	Family G	Moghadam *et al.* 2020	-